NATIONAL ADVISORY COMMITTEE FOR AERONAUTICS

TECHNICAL NOTE 2315

SUPERSONIC LIFT AND PITCHING MOMENT OF THIN SWEPTBACK

TAPERED WINGS PRODUCED BY CONSTANT

VERTICAL ACCELERATION

SUBSONIC LEADING EDGES AND SUPERSONIC TRAILING EDGES

By Frank S. Malvestuto, Jr., and Dorothy M. Hoover

Langley Aeronautical Laboratory
Langley Field, Va.

NACA

NATIONAL ADVISORY COMMITTEE FOR AERONAUTICS

TECHNICAL NOTE 2315

SUPERSONIC LIFT AND PITCHING MOMENT OF THIN SWEPTBACK

TAPERED WINGS PRODUCED BY CONSTANT

VERTICAL ACCELERATION

SUBSONIC LEADING EDGES AND SUPERSONIC TRAILING EDGES

By Frank S. Malvestuto, Jr., and Dorothy M. Hoover

SUMMARY

Theoretical approximations to the nondimensional lift and pitching moment produced by constant vertical acceleration, the $C_{L_{\dot{\alpha}}}$ and $C_{m_{\dot{\alpha}}}$ derivatives, respectively, are derived for a series of thin sweptback tapered wings with streamwise tips. The analysis is essentially the application of a recently published solution of the linearized time-dependent wave equation for wings in accelerated motion. The results are independent of camber and thickness and are applicable for a range of supersonic speed for which the wing is wholly contained between the Mach cones springing from the wing apex and from the trailing edge of the root section (subsonic leading edge and supersonic trailing edge).

Design curves are presented which permit rapid estimation of the derivatives $C_{L_{\dot{\alpha}}}$ and $C_{m_{\dot{\alpha}}}$ for given values of aspect ratio, taper ratio, Mach number, and leading-edge sweep.

INTRODUCTION

The formulations of linearized supersonic aerodynamics have allowed the theoretical derivation of many of the important longitudinal- and lateral-stability derivatives of various wing configurations. Recently, attention has been focused on the sweptback tapered wing with wing tips parallel to the wing plane of symmetry (hereinafter referred to as the "sweptback tapered wing"). Available stability derivatives for this wing for a wide range of Mach number now include the lift-curve slope $C_{L_{\alpha}}$, references 1 to 3; the damping-in-roll derivative C_{l_p}, references 2 to 4; the lateral-force and yawing-moment derivatives C_{Y_p} and C_{n_p},

respectively, references 5 and 6; and the longitudinal derivatives C_{m_α} (pitching moment due to angle of attack), C_{L_q} (lift due to pitching), and C_{m_q} (damping in pitch), reference 7.

The present paper is an extension of the previous investigations dealing with the sweptback tapered wing traveling at supersonic speeds and is concerned with the lift and the pitching moment resulting from constant vertical acceleration, the $C_{L_{\dot\alpha}}$ and $C_{m_{\dot\alpha}}$ derivatives, respectively. Theoretical expressions are derived herein which approximate with practical accuracy these two acceleration derivatives.

Basically, the analysis depends upon the solution of the linearized time-dependent wave equation for wings in accelerated motion reported by Gardner and by Watkins in references 8 and 9, respectively, and the application thereof to triangular wings in reference 10. The analyses of references 8 and 9 have in effect demonstrated that for a wing the time-dependent potential for constant vertical acceleration may be compounded of two time-free or steady-state potentials, one for angle of attack and the other for steady-state pitching. In terms of forces and moments, the analysis of reference 10 shows that such a decomposition of the time-dependent potential allows the derivatives $C_{L_{\dot\alpha}}$ and $C_{m_{\dot\alpha}}$ to be expressed in terms of the steady-state-pitching and angle-of-attack derivatives $\left(C_{L_q}, \ C_{m_q}, \text{ and } C_{m_\alpha}\right)$ plus additional terms dependent upon the surface velocity potential and corresponding pressure function for constant angle of attack. The results of reference 10 and the present results for the $C_{L_{\dot\alpha}}$ and $C_{m_{\dot\alpha}}$ derivatives are restricted to relatively slow rates of acceleration such as arise in the study of airplane stability. Approximate expressions for the derivatives C_{L_α}, C_{m_α}, C_{L_q}, and C_{m_q} for use in the evaluation of the derivatives of sweptback wings contained in this paper have previously been determined in references 3 and 7. Approximate expressions for the terms dependent upon the surface velocity potential and corresponding pressure distribution are derived herein.

The results of the analysis are applicable for a range of Mach number which allows the leading edge to be subsonic and the trailing edge to be supersonic with the additional trivial limitation that the Mach lines from the leading edge of the wing tip cannot intersect on the wing or intersect the opposite wing edges. Design curves are presented which permit rapid estimations of the derivatives $C_{L_{\dot\alpha}}$ and $C_{m_{\dot\alpha}}$ for given values of aspect ratio, taper ratio, Mach number, and leading-edge sweep.

SYMBOLS

x,y,z Cartesian coordinates of an arbitrary point

u_i,v_i,w_i induced flow velocities along x, y, and z body axes, respectively (see fig. 2(a))

u,v,w incremental flight velocities along x, y, and z stability axes, respectively (see fig. 2(b))

X,Y,Z forces parallel to x-, y-, z-axes, respectively

V flight speed

α angle of attack (w/V)

$\dot{\alpha}$ rate of change of α with time $(d\alpha/dt)$

q pitching velocity about y-axis

M stream Mach number $(V/\text{Speed of sound})$

μ Mach angle

B cotangent of Mach angle $\left(\sqrt{M^2 - 1}\right)$

ϵ angle between leading edge and axis of wing symmetry (see fig. 1(a))

λ taper ratio of wing

Λ leading-edge sweep $(90^{\circ} - \epsilon)$

$\theta_0 = \tan \epsilon$

δ angle between trailing edge and axis of symmetry (see fig. 1(a))

$m = \dfrac{\tan \epsilon}{\tan \mu} = \theta_0 B$

ω geometric parameter of wing $\left(\dfrac{2c_r\theta_0}{b} = \dfrac{4\theta_0}{A(1 + \lambda)} = \dfrac{4m}{AB(1 + \lambda)}\right)$

$n = \dfrac{\tan \epsilon}{\tan \delta} = 1 - (1 - \lambda)\omega$

$\nu = \dfrac{y}{x\theta_0}$

b   wing span

$\bar{x}$ x-component of center-of-gravity position

c_r wing root chord

c   over-all length

$\bar{c}$ mean aerodynamic chord $\left(\dfrac{2}{S} \displaystyle\int_0^{b/2} (\text{Local chord})^2 dy = \dfrac{2c_r \left[3\omega^2 - 3\omega(1 - n) + (1 - n)^2 \right]}{3\omega^2(1 + \lambda)} \right)$

l distance of leading edge of local wing chord behind apex of
            wing

S   wing area

A   aspect ratio of wing

ψ steady-state potential corresponding to a unit pitching
            velocity about y-axis

χ steady-state potential corresponding to unit angle of attack

ϕ perturbation velocity potential on upper surface of wing

t   time

a   speed of sound

ρ density of air

ΔP local pressure difference between lower and upper surfaces of
            airfoil, positive in sense of lift

$(\Delta P)_{q=1}$ lift distribution for unit pitching velocity

$(\Delta P)_{\alpha=1}$ lift distribution for unit angle of attack

C_P pressure coefficient $\left(\dfrac{\Delta P}{\frac{1}{2}\rho V^2} \right)$

M'   pitching moment

C_m pitching-moment coefficient $\left(\dfrac{M'}{\frac{1}{2}\rho V^2 S\bar{c}}\right)$

C_L lift coefficient $\left(\dfrac{\text{Lift}}{\frac{1}{2}\rho V^2 S}\right)$

$C_{m_\alpha} = \left(\dfrac{\partial C_m}{\partial \alpha}\right)_{\alpha \to 0}$

$C_{L_q} = \left(\dfrac{\partial C_L}{\partial \frac{q\bar{c}}{2V}}\right)_{q \to 0}$

$C_{m_q} = \left(\dfrac{\partial C_m}{\partial \frac{q\bar{c}}{2V}}\right)_{q \to 0}$

$\left(C_{L_{\dot\alpha}}\right)_1 = C_{L_q} + 2C_{m_\alpha}$

$\left(C_{L_{\dot\alpha}}\right)_2 = \dfrac{8}{S\bar{c}} \iint_{\text{Wing}} \dfrac{\chi}{V}\, dS$

$C_{L_{\dot\alpha}} = \left(\dfrac{\partial C_L}{\partial \frac{\dot\alpha\bar{c}}{2V}}\right)_{\dot\alpha \to 0} = \dfrac{M^2}{B^2}\left(C_{L_{\dot\alpha}}\right)_1 - \dfrac{1}{B^2}\left(C_{L_{\dot\alpha}}\right)_2$

$\left(C_{m_{\dot\alpha}}\right)_1 = C_{m_q} + \dfrac{2}{S\bar{c}^2} \iint_{\text{Wing}} x^2 \left(\dfrac{\Delta P}{\frac{1}{2}\rho V^2}\right)_{\alpha=1} dS$

$\left(C_{m_{\dot\alpha}}\right)_2 = -\dfrac{8}{S\bar{c}^2} \iint_{\text{Wing}} x\, \dfrac{\chi}{V}\, dS$

$C_{m_{\dot\alpha}} = \left(\dfrac{\partial C_m}{\partial \frac{\dot\alpha\bar{c}}{2V}}\right)_{\dot\alpha \to 0} = \dfrac{M^2}{B^2}\left(C_{m_{\dot\alpha}}\right)_1 - \dfrac{1}{B^2}\left(C_{m_{\dot\alpha}}\right)_2$

$k = \sqrt{1 - m^2}$

E'(m)   complete elliptic integral of the second kind with modulus k

$$\left(\int_0^{\pi/2} \sqrt{1 - k^2\sin^2 z}\ dz \right)$$

$E''(m) = \frac{1}{E'(m)}$ (see fig. 3)

When x, y, and t are used as subscripts, the respective partial derivative is indicated. For example,

$$\phi_x = \frac{\partial\phi}{\partial x}; \qquad \phi_{xt} = \frac{\partial^2\phi}{\partial x\ \partial t}$$

Primed symbols X', $\Delta P'$, and ϕ' refer to the wing-tip region shown in figure 1.

ANALYSIS

Scope

The sweptback wings considered in this paper are sketched in fig-ure 1. In the following analysis, the plan form with sweptback trailing edge (fig. 1(a)) is generally considered to be the typical wing, but the results of the analysis are equally valid for the wing plan form with the sweptforward trailing edge (fig. 1(b)). The orientation of the wing with respect to a body system of coordinate axes used in the analysis is indicated in figure 2(a). The surface velocity potential, the basic pressure distribution, and the stability derivatives are derived with respect to this system. Figure 2(b) shows the wing orientated with respect to the stability axes system with the origin of the system at the arbitrary location ($\bar{x}$, 0, 0) rearward of the apex of the wing. The transformation formulas that allow the determination of the derivatives with respect to the stability system once they are evaluated with respect to the body axes system are presented in table I.

The analysis is limited to wings having small thickness and camber and that are not yawed with respect to the free-stream direction. The derivatives are valid only for a range of supersonic speed which allows the leading edge to be subsonic and the trailing edge to be supersonic. The terms "subsonic leading edge" and "supersonic trailing edge" refer to the conditions that the Mach number of the stream component normal to the leading edge is less than 1 and that the Mach number of the stream component normal to the trailing edge is greater than 1, respectively. An additional trivial restriction is that the Mach lines emanating from

the wing tips cannot intersect on the wing. These conditions, expressed
mathematically as restrictions for $B \cot \Lambda$, are as follows: For
$BA(1 + \lambda) = 2$

$$\frac{BA(1 + \lambda)}{BA(1 + \lambda) + 4(1 - \lambda)} \leqq B \cot \Lambda \leqq 1$$

and for $BA(1 + \lambda) < 2$

$$\frac{BA(1 + \lambda)}{BA(1 + \lambda) + 4(1 - \lambda)} \leqq B \cot \Lambda \leqq \frac{BA(1 + \lambda)}{4 - BA(1 + \lambda)}$$

Basic Considerations

The derivation of the derivatives $C_{L_{\dot{\alpha}}}$ and $C_{m_{\dot{\alpha}}}$ basically depends
upon the solution of the linearized potential equation for time-
dependent motion

$$B^2 \phi_{xx} - \phi_{yy} + \frac{2V}{a^2} \phi_{xt} + \frac{1}{a^2} \phi_{tt} = 0 \qquad (1)$$

required to fulfill the boundary condition on the wing (approximately
in the $z = 0$ plane)

$$\frac{\partial \phi}{\partial z} = -\dot{\alpha} V t$$

It was reported in the section of the analysis of reference 10
dealing with the acceleration derivatives of triangular wings that
Gardner has, in effect, shown that a proper solution of equation (1) is

$$\frac{\phi}{\dot{\alpha}} = \frac{M^2}{B^2} \psi + \left(t - \frac{M^2 x}{VB^2} \right) \chi \qquad (2)$$

where ψ is the steady-state potential corresponding to a unit pitching
velocity about the y-axis and χ is the steady-state potential corre-
sponding to a unit angle of attack. Thus, the solution by Gardner and
an essentially equivalent solution by Watkins (reference 9) allow the
time-dependent potential for an angle of attack $\dot{\alpha} t$ to be expressed in
terms of two time-independent or steady-state potentials, one for a
constant angle of attack and the other for steady pitching. The appli-
cation of the solution expressed in equation (2) permits with relative
ease the evaluation of the pressure distribution for vertical motion
with constant acceleration. The corresponding derivatives $C_{L_{\dot{\alpha}}}$ and $C_{m_{\dot{\alpha}}}$

may then be derived rather simply in terms of integral expressions of the surface velocity potential and surface pressure distribution for constant unit angle of attack together with terms involving the non-dimensional forces and moments associated with angle of attack and steady pitching. The general formal levelopment of the derivatives $C_{L_{\dot{\alpha}}}$ and $C_{m_{\dot{\alpha}}}$ based upon the velocity potential expression of equation (2) has been carried out in reference 10. Adhering to the analysis in that paper, the lifting-pressure distribution at time $t = 0$ for the angle of attack $\dot{\alpha}t$ is obtained from the surface velocity potential by

$$\Delta P = 2\rho\left(V\phi_x + \phi_t\right)_{t=0}$$

$$= 2\rho V\dot{\alpha}\left(\frac{M^2}{B^2}\psi_x - \frac{M^2 x}{VB^2}\chi_x - \frac{X}{VB^2}\right)$$

$$= \frac{\dot{\alpha}}{B^2}\left[M^2(\Delta P)_{q=1} - \frac{M^2 x}{V}(\Delta P)_{\alpha=1} - 2\rho X\right] \qquad (3)$$

where $(\Delta P)_{q=1}$ is the lift distribution for unit pitching velocity about the y-axis and $(\Delta P)_{\alpha=1}$ is the lift distribution for unit angle of attack. The choice of time $t = 0$ eliminates the lift due to angle of attack and leaves only the increment due to time rate of change of angle of attack.

Integration of equation (3) to obtain the lift and moment and reduction to coefficient forms yields

$$C_{L_{\dot{\alpha}}} = \frac{M^2}{B^2}C_{L_q} + \frac{2M^2}{B^2}C_{m_\alpha} - \frac{8}{B^2 S\bar{c}}\iint\frac{X}{V}\,ds \qquad (4)$$

$$C_{m_{\dot{\alpha}}} = \frac{M^2}{B^2}C_{m_q} + \frac{2M^2}{B^2 S\bar{c}^2}\iint x^2\left(\frac{\Delta P}{\frac{1}{2}\rho V^2}\right)_{\alpha=1}dS + \frac{8}{B^2 S\bar{c}^2}\iint x\frac{X}{V}\,dS \qquad (5)$$

where the integrations are performed over the wing plan form. For convenience, the following symbols will be used:

$$\left(C_{L_{\dot{\alpha}}}\right)_1 = C_{L_q} + 2C_{m_\alpha}$$

$$\left(C_{L_{\dot{\alpha}}}\right)_2 = \frac{8}{S\bar{c}} \iint \frac{X}{V} \, dS$$

so that

$$C_{L_{\dot{\alpha}}} = \frac{M^2}{B^2}\left(C_{L_{\dot{\alpha}}}\right)_1 - \frac{1}{B^2}\left(C_{L_{\dot{\alpha}}}\right)_2$$

and, similarly,

$$\left(C_{m_{\dot{\alpha}}}\right)_1 = C_{m_q} + \frac{2}{S\bar{c}^2} \iint x^2 \left(\frac{\Delta P}{\frac{1}{2}\rho V^2}\right)_{\alpha=1} \, dS$$

$$\left(C_{m_{\dot{\alpha}}}\right)_2 = -\frac{8}{S\bar{c}^2} \iint x \, \frac{X}{V} \, dS$$

so that

$$C_{m_{\dot{\alpha}}} = \frac{M^2}{B^2}\left(C_{m_{\dot{\alpha}}}\right)_1 - \frac{1}{B^2}\left(C_{m_{\dot{\alpha}}}\right)_2$$

Satisfactory approximate expressions for the derivatives C_{m_α}, C_{L_q}, and C_{m_q} that occur in equations (4) and (5) for $C_{L_{\dot{\alpha}}}$ and $C_{m_{\dot{\alpha}}}$, respectively, have previously been determined and presented in reference 7 for the wing plan forms and Mach number range considered in this paper. The double integral terms remain to be evaluated for a complete estimation of $C_{L_{\dot{\alpha}}}$ and $C_{m_{\dot{\alpha}}}$. These integrals and the approximate expressions therein for the potential X and the pressure $(\Delta P)_{\alpha=1}$ are considered in the following sections.

Expressions for the integrals $\iint \frac{X}{V} \, dS$ and $\iint x \, \frac{X}{V} \, dS$.- An approximation to the steady-state surface velocity potential of a sweptback wing at a unit angle of attack has been derived in reference 3. The entire approximation occurs in the expression for the surface velocity potential for the region of the wing internal to the Mach cones from the leading edge of the wing tips. For the region of the wing external to the wing-tip Mach cones, the velocity potential distribution is exact and is the same as the linearized potential distribution for the corresponding part of a triangular wing for the same leading-edge sweep and Mach number.

The surface velocity potential for the triangular wing may be derived
from the analysis of reference 11 and is expressed as follows for the
upper surface of the wing for unit angle of attack:

$$\chi = \frac{\phi}{\alpha} = \frac{V\sqrt{\theta_o^2 x^2 - y^2}}{E'(m)}$$

or

$$\chi = \frac{V\theta_o x\sqrt{1 - \nu^2}}{E'(m)} \tag{6}$$

where ν is a conical coordinate $y/\theta_o x$ proportional to the slope of
a ray from the apex of the wing and $E'(m)$ is the complete elliptic
integral of the second kind dependent upon $m = \dfrac{\tan \epsilon}{\tan \mu}$. The variation
of $\dfrac{1}{E'(m)}$ with m is presented in figure 3. From reference 3, the
corresponding approximate expression for the potential of the wing-tip
region is given by

$$\chi' = \frac{\phi'}{\alpha} = \frac{2V}{\pi}\sqrt{\frac{2(mx + By)(b - 2y)}{B(1 + m)}} \tag{7}$$

The approximate surface velocity potential for the entire wing for a
unit angle of attack is then the sum of the expressions (6) and (7).
The integral terms of equations (4) and (5) containing χ may now be
expressed in the following form (see fig. 4 for regions):

$$\frac{8}{B^2 S\bar{c}} \iint_{\text{Wing}} \frac{\chi}{V} \, dS = \frac{16\theta_o}{B^2 S\bar{c}E'(m)} \iint_{\substack{\text{Region} \\ \text{oegh}}} x\sqrt{1 - \nu^2} \, dS +$$

$$\frac{32\sqrt{2}}{\pi B^2 S\bar{c}\sqrt{B(1 + m)}} \iint_{\substack{\text{Region} \\ \text{efg}}} \sqrt{(mx + By)(b - 2y)} \, dS \tag{8}$$

and

$$\frac{8}{B^2 S\bar{c}^2} \iint_{\text{Wing}} x \frac{X}{V} \, dS = \frac{16\theta_0}{B^2 S\bar{c}^2 E'(m)} \iint_{\substack{\text{Region} \\ \text{oegh}}} x^2 \sqrt{1 - v^2} \, dS +$$

$$\frac{32\sqrt{2}}{\pi B^2 S\bar{c}^2 \sqrt{B(1 + m)}} \iint_{\substack{\text{Region} \\ \text{efg}}} x \sqrt{(mx + By)(b - 2y)} \, dS$$

$$(9)$$

The quasi-conical nature of the integrands (that is, of the form $x^n f(v)$ of the first integrals of the right-hand side of equations (8) and (9) allows these integrals to be easily evaluated by use of the "triangular" integration procedure considered in reference 12. When this procedure is used, the integrand $x\sqrt{1 - v^2} \, dS$ may be written as

Region ohgo	Region ogeo
$\dfrac{1}{3} c_r^3 \theta_0 \dfrac{\sqrt{1 - v^2}}{(1 - nv)^3} \, dv$	$\dfrac{1}{24} \dfrac{(1 + m)^3 b^3}{\theta_0^2} \dfrac{\sqrt{1 - v^2}}{(1 + mv)^3} \, dv$

and, similarly, the integrand $x^2 \sqrt{1 - v^2} \, dS$ becomes

Region ohgo	Region ogeo
$\dfrac{1}{4} c_r^4 \theta_0 \dfrac{\sqrt{1 - v^2}}{(1 - nv)^4} \, dv$	$\dfrac{1}{64} \dfrac{(1 + m)^4 b^4}{\theta_0^3} \dfrac{\sqrt{1 - v^2}}{(1 + mv)^4} \, dv$

Equations (8) and (9) are now conveniently expressed as follows:

$$\frac{8}{B^2 S\bar{c}} \iint \frac{x}{V}\, dS = \frac{16\theta_c^2 c_r^3}{3B^2 S\bar{c}E'(m)} \int_0^{\frac{1-\omega+m}{(1+m)n+m\omega}} \frac{\sqrt{1-\nu^2}}{(1-m\nu)^3}\, d\nu + \frac{2(1+m)^3 b^3}{3B^2 \theta_0 S\bar{c}E'(m)} \int_{\frac{1-\omega+m}{(1+m)n+m\omega}}^1 \frac{\sqrt{1-\nu^2}}{(1+m\nu)^3}\, d\nu +$$

$$\frac{32\sqrt{2}}{\pi B^2 S\bar{c}\sqrt{B(1+m)}} \int_0^{b/2} \int_{\frac{1+m-\omega}{n+m}\frac{b}{2}}^{c_r+\frac{yn}{\theta_0}} \frac{1+m}{2}\frac{b}{2}-yB \sqrt{(mx+By)(b-2y)}\, dx\, dy \qquad (10)$$

and

$$\frac{8}{B^2 S\bar{c}^2} \iint x\, \frac{x}{V}\, dS = \frac{4\theta_0^2 c_r^4}{B^2 S\bar{c}^2 E'(m)} \int_0^{\frac{1-\omega+m}{(1+m)n+m\omega}} \frac{\sqrt{1-\nu^2}}{(1-n\nu)^4}\, d\nu + \frac{(1+m)^4 b^4}{4B^2 \theta_0^2 S\bar{c}^2 E'(m)} \int_{\frac{1-\omega+m}{(1+m)n+m\omega}}^1 \frac{\sqrt{1-\nu^2}}{(1+m\nu)^4}\, d\nu +$$

$$\frac{32\sqrt{2}}{\pi B^2 S\bar{c}^2 \sqrt{B(1+m)}} \int_0^{b/2} \int_{\frac{1+m-\omega}{n+m}\frac{b}{2}}^{c_r+\frac{yn}{\theta_0}} \frac{1+m}{2}\frac{b}{2}-yB\ x\sqrt{(mx+By)(b-2y)}\, dx\, dy \qquad (11)$$

Evaluation of the integrals in expressions (10) and (11) yields for the entire wing the following expressions for $\dfrac{8}{B^2 S\bar{c}} \iint \dfrac{x}{V}\, dS$ and $\dfrac{8}{B^2 S\bar{c}^2} \iint x\, \dfrac{x}{V}\, dS$ in terms of the wing parameters m, n, A, and ω:

$$\frac{8}{\beta^2 S \overline{C}} \iint \frac{x}{V} \, dS = \frac{1}{\beta^2} \left(C_{L\alpha}\right)_2$$

$$= \frac{4m}{\beta^3 \left[3\omega^2 - 3\omega(1-n) + (1-n)^2\right]} \left\{ \frac{2m(m^2-1)(n^2-1) + (1+nm)\omega^2(m-1) + (1+m)(n^2-1)}{(n^2-1)(m-1)(n+m)^2} \sqrt{\left[(1+m)(1+n) + \omega(m-1)\right]\left[(\omega+n-1)(1+m)\right]} + \right.$$

$$\frac{\omega^3}{(n^2-1)\sqrt{1-n^2}} \left[\sin^{-1} \frac{(1+m)(n^2-1) + \omega(1+nm)}{n(m+n)} - \sin^{-1} n \right] - \frac{nm^3}{n^2-1} \left[\frac{\sin^{-1} \frac{\omega(1-m) - (nm+1)}{n+m}}{(1-m)^{3/2}} + \frac{\pi}{2} \right] + \left. \right.$$

$$\frac{8}{\pi \sqrt{1+m}} (m-1)(1+n+\omega)\left[2(1+m-\omega) - (1+n-\omega)(n+m)\right]\sqrt{\left[(1+m)(1+n) + \omega(m-1)\right]\left[(\omega+n-1)(1+m)\right]} + 4(1+n)\left[(1+m)(1+n) + \omega(m-1)\right]^2 \right.$$

$$\frac{(1+n+\omega)^3}{8(1+m)(n+m)^2}\left[\frac{\sin^{-1}\frac{\omega(n-1) - (1+nm)}{(1+n+\omega)(n+m)} - 2(1+n)(1+n+m-\omega)}{(1-m)^{3/2}} - \frac{1}{(1-m)^{3/2}} \sin^{-1}\frac{\omega(m-1) - (1+nm)}{n+m} + \frac{\pi}{2} \right\} \tag{12a}$$

For $m = 1$, the Mach lines from the wing apex coincide with the leading edges of the wing. Then equation (12a) becomes

$$\frac{1}{\beta^2}\left(C_{L\alpha}\right)_2 = \frac{16}{\pi\beta^3(n+1)\left[3\omega^2 - 3\omega(1-n) + (1-n)^2\right]}\left\{ \frac{1}{3}\left[2(n-1)\left[7\omega + 4(n-1)\right] + 3\omega^2}{3\sqrt{1+n}} + \frac{\omega^3}{2\sqrt{1-n^2}}\left[\sin^{-1}\frac{2(n-1) + \omega}{\omega+n-1} - \sin^{-1}n\right] - \frac{n m^3}{2} \right\} \tag{12b}$$

$$\frac{8}{\beta^2 S \overline{C}^2} \iint \frac{x}{V} \, dS = -\frac{1}{\beta^2}\left(C_{m\alpha}\right)_2$$

$$= \frac{8}{\pi\sqrt{1+n}}\left\{ \frac{\sqrt{(\omega+n-1)^3}}{3} - (\omega+n-3)\sqrt{2(\omega+n-1)} - \frac{(1+n+\omega)^2}{2}\left(\sin^{-1}\frac{\omega+n-3}{1+n+\omega} + \frac{\pi}{2}\right) \right\} \tag{13a}$$

$$= \frac{6m^2}{AB^4\left[3\omega^2 - 3\omega(1-n) + (1-n)^2\right]^2}\left\{ \frac{1}{3(n^2-1)^3(m-1)^3(m+1)^{3/2}(m+n)^3}\left[(1-\omega+m)^2\left[\omega(m-1)^3(m+1)^2(-2n^5+n^3+n) - (n^2-1)^3(2m^5-m^3-m) + \right.\right.$$

... (continued)

$$\text{For } m = 1, \text{ equation (13a) becomes}$$

$$-\frac{1}{\beta^2}\left(C_{m\alpha}\right)_2 = \frac{24}{\pi AB^4(n+1)^{5/2}\left[3\omega^2 - 3\omega(n-1) + (1-n)^2\right]^2}\left\{ \frac{3}{(n-1)^3\sqrt{1+n}}\left[(2-\omega)^2\left[5\omega(n+n^3-2n^5) - 4(n^2-1)^3\right] + (2n+\omega)(2-\omega)\left[5\omega(3n^4-3) - 12(n^2-1)^3\right] + (2n+\omega)^2\left[5\omega(2n^5-7n^3+5n) + 16(n^2-1)^3\right]}{15(1+n)^{5/2}} \right.$$

$$\left. + \frac{\omega^4\sqrt{1-n^2}}{2}\left[\sin^{-1}\frac{2(n-1) + \omega}{\omega+n-1} - \sin^{-1}n\right] - \frac{\omega^4(2n^5 - 7n^3 + 5n)}{3(n^2-1)^3} - \right.$$

$$\left. \frac{(1+n+\omega)^2}{2}\left[\sin^{-1}\frac{(-3+\omega+n)}{(1+n+\omega)} + \frac{\pi}{2}\right] \right\} \tag{13b}$$

Expression for the integral $\iint x^2 \left(\dfrac{\Delta P}{\frac{1}{2}\rho V^2}\right)_{\alpha=1} dS.$ – The evaluation of

the integral $\iint x^2 \left(\dfrac{\Delta P}{\frac{1}{2}\rho V^2}\right)_{\alpha=1} dS$ necessitates a knowledge of the lifting

pressure for the wing at an angle of attack. For the region of the wing external to the wing-tip Mach cones, the pressure distribution is merely the exact linearized pressure distribution for the corresponding part of the triangular wing for the same value of leading-edge sweep and Mach number. From reference 11, the following expression may be obtained for the lifting-pressure coefficient for a unit angle of attack

$$\left(\frac{\Delta P}{\frac{1}{2}\rho V^2}\right)_{\alpha=1} = \frac{4\theta_0^2 x}{E'(m)\sqrt{\theta_0^2 x^2 - y^2}}$$

or, in terms of the conical coordinate $\nu = \dfrac{y}{\theta_0 x}$,

$$\left(\frac{\Delta P}{\frac{1}{2}\rho V^2}\right)_{\alpha=1} = \frac{4\theta_0}{E'(m)\sqrt{1 - \nu^2}} \tag{14}$$

The corresponding expression for the approximate lifting-pressure distribution for the region of the wing internal to the wing-tip Mach cones has been derived in reference 3. From therein, the lifting-pressure coefficient for unit angle of attack is as follows:

$$\left(\frac{\Delta P'}{\frac{1}{2}\rho V^2}\right)_{\alpha=1} = \frac{8}{\pi}\sqrt{\frac{\theta_0}{1 + B\theta_0}}\sqrt{\frac{\frac{b}{2} - y}{x + \frac{y}{\theta_0}}} \tag{15}$$

Substitution of the sum of the component pressures expressed by equations (14) and (15) for $\left(\dfrac{\Delta P}{\frac{1}{2}\rho V^2}\right)_{\alpha=1}$ of the integral to be evaluated yields

$$\iint_{\text{Wing}} x^2 \left(\frac{\Delta P}{\frac{1}{2}\rho V^2}\right)_{\alpha=1} dS = \frac{8\theta_o}{E'(m)} \iint_{\substack{\text{Region}\\\text{oegh}}} \frac{x^2}{\sqrt{1-\nu^2}}\, dS + \frac{16}{\pi} \iint_{\substack{\text{Region}\\\text{efg}}} x^2 \sqrt{\frac{\theta_o}{1+B\theta_o}} \sqrt{\frac{\frac{b}{2}-y}{x+\frac{y}{\theta_o}}}\, dS \quad (16)$$

The first integral of the right-hand side of equation (16) represents the contribution of the part of the wing external to the wing-tip Mach cones. This integral, because of the $x^n f(\nu)$ form of the integrand, may be resolved into a single integral by the triangular integration procedure considered previously. The integrand $\dfrac{x^2}{\sqrt{1-\nu^2}}$ becomes

Region ohgo

$$\frac{1}{4}\,\frac{\frac{c_r^4}{4}\theta_o}{(1-n\nu)^4 \sqrt[4]{1-\nu^2}}$$

Region ogeo

$$\frac{1}{64}\,\frac{(1+m)^4 b^4}{\theta_o^3(1+m\nu)^4 \sqrt[4]{1-\nu^2}} \quad (17)$$

The results given by expressions (16) and (17) allow the integral term $\dfrac{2M^2}{B^2 S\bar{c}^2} \displaystyle\iint x^2 \left(\frac{\Delta P}{\frac{1}{2}\rho V^2}\right)_{\alpha=1} dS$ of equation (5) to be expressed in the following form:

$$\frac{2M^2}{B^2 S\bar{c}^2} \iint x^2 \left(\frac{\Delta P}{\frac{1}{2}\rho V^2}\right)_{\alpha=1} dS = \frac{2M^2}{B^2}\sqrt{\frac{2\theta_o^2 c_r^4}{S\bar{c}^2 E'(m)}}\left[\int_0^{\frac{1-\omega+m}{(1+m)n+m\omega}} \frac{d\nu}{(1-n\nu)^4 \sqrt[4]{1-\nu^2}} + \frac{(1+m)^4 b^4}{8\theta_o^2 S\bar{c}^2 E'(m)} \int_{\frac{1-\omega+m}{(1+m)n+m\omega}}^{1} \frac{d\nu}{(1+m\nu)^4 \sqrt[4]{1-\nu^2}}\right] +$$

$$\frac{32\theta_o M^2}{\pi B^2 S\bar{c}^2 \sqrt{2}\sqrt{1+\frac{1+m-\omega}{n+m}}}\int_{\frac{1+m-\omega}{n+m}\frac{b}{2}}^{b/2}\int_0^{c_r+\frac{yn}{\theta_o}} x^2 \sqrt{\frac{\frac{b}{2}-2y}{\theta_o x + y}}\;dx\,dy \quad (18)$$

Evaluation of the integrals of equation (18) yields the following expression for $\dfrac{2M^2}{B^2 S\bar{c}^2}\displaystyle\iint x^2 \left(\frac{\Delta P}{\frac{1}{2}\rho V^2}\right)_{\alpha=1} dS$ in terms of m, n, A, and ω:

$$\frac{2M^2}{\beta^2 S c^2} \iint x^2 \left(\frac{\Delta P}{\frac{1}{2}\rho V^2}\right) dS = \frac{2M^2}{\beta^2} \left\{ \frac{3m^2}{AB^2}\left[3\omega^2 - 3\omega(1-n) + (1-n)^2\right]^2 \left\{ \frac{1}{B^2(m)}\left[3(m+n)^3(n^2-1)^3(m-1)^3(m+1)^{3/2}\left[(1-\omega+m)^2\left[\omega(m-1)^3(m+1)^3(11n^3+4n^5)+(n^2-1)^3(11n^3+4n^5)\right]-\left[(1+m)n+\right.\right.\right.\right.$$

$$m\omega\right][(1-\omega+m)\left[\omega(m-1)^3(m+1)^2(27n^2+3n^4)-(n^2-1)^3(27n^2+3n^4)\right]+\left[(1+m)n+m\omega\right]^2\left[\omega(m-1)^3(m+1)^2(2n^5-5n^3+18n)-(n^2-1)^3(5n^3-18n-2m^5)\right]\right\}\sqrt{(1+m)(1+n)+\omega(m-1)}\right](\omega+n-1)-$$

$$\frac{\omega^4(2n^5-5n^3+18n)}{3(n^2-1)^3}+\frac{\omega^4(3n^2+2)}{(n^2-1)^3}\sqrt{\frac{1+m}{1-n^2}}\left[\frac{\sin^{-1}\frac{(n^2-1)(1+m)+\omega(1+nm)}{\omega(m+n)}-\sin^{-1}n}{(1-n)^{7/2}}\right]+\frac{(3m^2+2)\sqrt{\frac{1+m}{2}}\left[\sin^{-1}\frac{\omega(1-m)-(1+m)}{n+m}+\frac{\pi}{2}\right]}{(1-m)^{7/2}}+$$

$$\frac{4}{5\pi\sqrt{1+m}}\left[\frac{(1-m)^2(n+m)\left[5(1+n-\omega)(8-4m+3n^2)-16\omega(1+n)(2-3n)\right]+6(1+n)(1-m)(1+m-\omega)\left[(1-m)(8-4n+3n^2)-(1+n)(8+4m+3n^2)\right]+2(1+n)^2(n+m)(16+64m+4m^2-9m^3)}{3(1+n)^2(1-m)^2(n+m)^4}\sqrt{(1+m)(1+n)+\omega(m-1)}\right]^{3/2}\left[\sqrt{(1+m)(1+n)+\omega(m-1)}\right]$$

$$\frac{5}{\sqrt{\frac{4\omega(1+n)(3n^2+4\omega)+(1+n-\omega)^2(8-4n+3n^2)}{8(1+n)^3}-\frac{2(1+n)(1+n-\omega)(n+m)}{-(n+m)^2}}}-$$

$$\frac{\omega(m-1)\left[(\omega+n-1)\right]^{3/2}-\frac{5(4+4m+7m^2)}{(1-m)^3}+\frac{(1+n+\omega)^2\sin^{-1}\frac{(1+n-\omega)(n+m)-2(1+n)(1+m-\omega)}{(1+n+\omega)(n+m)}+\frac{\pi}{2}}{2\sqrt{1+n}}}{-(n+m)^2}$$

$$\frac{(1+n+\omega)^2}{2\sqrt{1+n}}\sin^{-1}\frac{(1+n-\omega)(n+m)-2(1+n)(1+m-\omega)}{(1+n+\omega)(n+m)}+\frac{\pi}{2}-\sqrt{\frac{(1+m)(1+n)+\omega(m-1)}{-(n+m)^2}}\left[\sqrt{(1+m)(1+n)+\omega(m-1)}\right](\omega+n-1)-\frac{1}{\sqrt{1-m}}\left[\frac{\sin^{-1}\frac{\omega(1-m)-(1+m)}{n+m}+\frac{\pi}{2}}{}\right]\left[\frac{}{}\right] \tag{19a}$$

For m = 1, the Mach lines from the wing apex coincide with the leading edges of the wing. Then equation (19a) becomes

$$\frac{2M^2}{\beta^2 S c^2}\iint x^2\left(\frac{\Delta P}{\frac{1}{2}\rho V^2}\right)dS = \frac{2M}{\beta^2}\left\{\frac{12}{\pi AB^2(n+1)^3}\left[3\omega^2-3\omega(1-n)+(1-n)^2\right]^2\sqrt{\frac{3}{(n-1)^3}}\left[\frac{35\omega(2n+\omega)\left[(2n^5-5n^3+18n)(2n+\omega)-(27n^2+3n^4)(2-\omega)\right]+(11n^3+4n^5)(2-\omega)^2}{105(n+1)^{5/2}}\right\}\sqrt{\omega+n-1}+$$

$$\frac{6(n-1)^3(n+1)^2\left[2(2-\omega)^2(2+8n+3\omega)+(2n+\omega)^2(26+24n-\omega)\right]}{105(n+1)^{5/2}}\sqrt{\omega+n-1}-\frac{\omega^4(3n^2+2)\left[\sin^{-1}\frac{2(n-1)+\omega}{\omega}-\sin^{-1}n\right]}{2\sqrt{1-n^2}}-\frac{\omega^4(2n^5-5n^3+18n)}{6}\right]+$$

$$\frac{2}{5\sqrt{1+n}}\left\{-\frac{(360\omega^2-216\omega+260n+136-36\omega n+199n^2-105n^3-105n^2\omega)(\omega+n-1)^{3/2}}{21}-\frac{5\left[(1+n-\omega)^2(8-4n+3n^2)+4\omega(1+n)(3n^2+4\omega)\right]}{16\sqrt{2}}\right.$$

$$\left.\left(3-\omega-n\right)\sqrt{2(\omega+n-1)}-\frac{(1+n+\omega)^2}{2}\left[\sin^{-1}\frac{(\omega+n-3)}{(\omega+n+1)}+\frac{\pi}{2}\right]\right\}\right\} \tag{19b}$$

RESULTS AND DISCUSSION

The preceding section involved the evaluation of the acceleration derivatives $C_{L_{\dot\alpha}}$ and $C_{m_{\dot\alpha}}$ as functions of the steady-state pitching derivatives $\left(C_{L_q},\ C_{m_\alpha},\ C_{m_q}\right)$ determined in reference 7 and the several integral terms determined herein which are functions of the surface velocity potential and the corresponding pressure distribution for constant unit angle of attack. The evaluation of these derivatives are approximate in that the contribution of the wing-tip region was obtained by use of an approximate surface velocity potential derived in references 3 and 7 by use of the point-source method of Evvard.

An indication of the lifting-pressure distribution over a typical wing (sketched in fig. 5) for three Mach line configurations can be obtained from figure 6. Figure 6(a) shows the pressure distribution for the case of a subsonic leading edge and a supersonic trailing edge; figure 6(b), for a subsonic leading edge and a sonic trailing edge; and figure 6(c), for a sonic leading edge and a supersonic trailing edge. As expected, a pronounced finite drop in the resultant lifting pressure occurs across the inboard Mach line from the wing tip. The resultant pressure distribution is generally negative for the wing plan form considered. For the Mach line configuration for which the leading edge is sonic and the trailing edge is supersonic (fig. 6(c)), the pressure along section a-a becomes slightly positive in the wing-tip region, in particular in the vicinity of the trailing edge. Results of additional computations for the variation of pressure loadings with aspect ratio indicate that, as the aspect ratio is decreased, the resultant pressures tend to become positive and eventually give rise to a positive (lifting) force $\left(C_{L_{\dot\alpha}}\right)$ and a stable nose-down pitching moment $\left(C_{m_{\dot\alpha}}\right)$; whereas, for the wing considered for figure 6, it is obvious that the integrated pressures will produce a negative $C_{L_{\dot\alpha}}$ and an unstable $C_{m_{\dot\alpha}}$.

The exact linearized solution for the lifting pressure in the wing-tip region induced by constant vertical acceleration is not available at present although extremely accurate approximations to the exact linearized solution that require laborious calculations may be obtained by the methods of reference 13. The present approximate method should be adequate for determining the integrated lift and pitching moment, especially since the pressures are relatively very small in the tip region where the approximations of the method apply. For a practical evaluation of the derivatives $C_{L_{\dot\alpha}}$ and $C_{m_{\dot\alpha}}$ it is believed that the wing-tip regions may be completely neglected.

A series of generalized curves that allow rapid estimation of the derivatives $C_{L_{\dot\alpha}}$ and $C_{m_{\dot\alpha}}$ is presented in figures 7 and 8, respectively.

For specified values of aspect ratio, taper ratio, Mach number, and

leading-edge sweep, the derivative $C_{L_{\dot{\alpha}}} = \frac{M^2}{B^2}\left(C_{L_{\dot{\alpha}}}\right)_1 - \frac{1}{B^2}\left(C_{L_{\dot{\alpha}}}\right)_2$ is esti-

mated from figure 7 and the derivative $C_{m_{\dot{\alpha}}} = \frac{M^2}{B^2}\left(C_{m_{\dot{\alpha}}}\right)_1 - \frac{1}{B^2}\left(C_{m_{\dot{\alpha}}}\right)_2$ is

estimated from figure 8. In figures 7 and 8, the segmental dashed parts
of the design curves to the left of the boundary lines labeled
"Sonic T.E." should be disregarded for estimations; they correspond to
conditions not treated in this paper, for which the trailing edge is
subsonic (Mach lines ahead of trailing edge) and hence allows trailing-
edge disturbances to affect the part of the wing bounded by the Mach
lines from the trailing-edge apex and trailing edge itself. These
dashed parts have been presented, however, to indicate the trend of the
variations and to act as an upper limit below which the true values of
the derivatives would lie for configurations for which the trailing edge
is subsonic. The boundary lines labeled "Sonic L.E." indicate the
other limit of validity for which the Mach lines coincide with the
leading edge.

It should be noted that the derivatives determined from the design
curves of figures 7 and 8 are with respect to a set of axes located at
the apex of the wing. The derivatives with respect to an arbitrary
center-of-gravity location ($x = \bar{x}$, $y = 0$, $z = 0$) in the stability axes
system may be easily obtained by transformation formulas presented in
table I.

Specific variations of the derivatives $C_{L_{\dot{\alpha}}}$ and $C_{m_{\dot{\alpha}}}$ (in the sta-
bility axes system) with each of the parameters - aspect ratio, taper
ratio, Mach number, and leading-edge sweep - are presented in figures 9
and 10, respectively. The variation of $C_{m_{\dot{\alpha}}}$ with aspect ratio plotted
in figure 10 shows the interesting point, mentioned previously in the
discussion of the pressure distributions of figure 6, that the pitching
moment which is generally unstable at the higher aspect ratios becomes
stable as the aspect ratio is decreased (below aspect ratio of approx. 2.25
for the illustrative case shown). Similar results have been noted for
the rectangular wing (reference 14), the triangular wing (reference 10),
and the sweptback wing of zero taper ratio (reference 12).

CONCLUDING REMARKS

Theoretical approximations to the nondimensional lift and pitching
moment produced by constant vertical acceleration, the $C_{L_{\dot{\alpha}}}$ and $C_{m_{\dot{\alpha}}}$
derivatives, respectively, have been derived for a series of thin

sweptback tapered wings with streamwise tips. Results are applicable
for a range of supersonic speed for which the wing is wholly contained
between the Mach cones springing from the wing apex and from the trailing
edge of the root section.

The results presented herein for the derivatives $C_{L_{\dot{\alpha}}}$ and $C_{m_{\dot{\alpha}}}$ are
applicable within the limitations of the linearized theory since the
approximation to the exact linearized solution in the wing-tip region
is satisfactory and this region has a minor effect on the values of the
derivatives for the entire wing.

Langley Aeronautical Laboratory
    National Advisory Committee for Aeronautics
        Langley Field, Va., December 22, 1950

REFERENCES

1. Cohen, Doris: The Theoretical Lift of Flat Swept-Back Wings at
     Supersonic Speeds. NACA TN 1555, 1948.

2. Harmon, Sidney M., and Jeffreys, Isabella: Theoretical Lift and
     Damping in Roll of Thin Wings with Arbitrary Sweep and Taper at
     Supersonic Speeds. Supersonic Leading and Trailing Edges. NACA
     TN 2114, 1950.

3. Malvestuto, Frank S., Jr., Margolis, Kenneth, and Ribner, Herbert S.:
     Theoretical Lift and Damping in Roll at Supersonic Speeds of Thin
     Sweptback Tapered Wings with Streamwise Tips, Subsonic Leading
     Edges, and Supersonic Trailing Edges. NACA Rep. 970, 1950.
     (Formerly NACA TN 1860.)

4. Walker, Harold J., and Ballantyne, Mary B.: Pressure Distribution
     and Damping in Steady Roll at Supersonic Mach Numbers of Flat Swept-
     Back Wings with Subsonic Edges. NACA TN 2047, 1950.

5. Harmon, Sidney M., and Martin, John C.: Theoretical Calculations of
     the Lateral Force and Yawing Moment Due to Rolling at Supersonic
     Speeds for Sweptback Tapered Wings with Streamwise Tips. Supersonic
     Leading Edges. NACA TN 2156, 1950.

6. Margolis, Kenneth: Theoretical Calculations of the Lateral Force and
     Yawing Moment Due to Rolling at Supersonic Speeds for Sweptback
     Tapered Wings with Streamwise Tips. Subsonic Leading Edges. NACA
     TN 2122, 1950.

7. Malvestuto, Frank S., Jr., and Hoover, Dorothy M.: Lift and Pitching
     Derivatives of Thin Sweptback Tapered Wings with Streamwise Tips
     and Subsonic Leading Edges at Supersonic Speeds. NACA TN 2294, 1951.

8. Gardner, C.: Time-Dependent Linearized Supersonic Flow past Planar
     Wings. Communications on Pure and Appl. Math., vol. III, no. 1,
     March 1950, pp. 33-38.

9. Watkins, Charles E.: Effect of Aspect Ratio on Undamped Torsional
     Oscillations of a Thin Rectangular Wing in Supersonic Flow. NACA
     TN 1895, 1949.

10. Ribner, Herbert S., and Malvestuto, Frank S., Jr.: Stability Deriva-
     tives of Triangular Wings at Supersonic Speeds. NACA Rep. 908, 1948.

11. Brown, Clinton E.: Theoretical Lift and Drag of Thin Triangular
     Wings at Supersonic Speeds. NACA Rep. 839, 1946.

12. Malvestuto, Frank S., Jr., and Margolis, Kenneth: Theoretical
      Stability Derivatives of Thin Sweptback Wings Tapered to a Point
      with Sweptback or Sweptforward Trailing Edges for a Limited Range
      of Supersonic Speeds. NACA Rep. 971, 1950. (Formerly NACA TN 1761.)

13. Mirels, Harold: Lift-Cancellation Technique in Linearized Supersonic-
      Wing Theory. NACA TN 2145, 1950.

14. Harmon, Sidney M.: Stability Derivatives at Supersonic Speeds of
      Thin Rectangular Wings with Diagonals ahead of Tip Mach Lines.
      NACA Rep. 925, 1949. (Formerly NACA TN 1706.)

TABLE I

TRANSFORMATION FORMULAS FROM BODY AXES TO STABILITY AXES

FOR STABILITY DERIVATIVES $C_{L_{\dot\alpha}}$ AND $C_{m_{\dot\alpha}}$

	Principal body axes (origin at $x = 0$, $y = 0$, $z = 0$)	Principal body axes (origin at $x = \bar{x}$, $y = 0$, $z = 0$)	Stability axes (origin at $x = \bar{x}$, $y = 0$, $z = 0$)	
	Stability derivative (1)	Shift in origin from (0,0,0) to ($\bar{x}$,0,0)	Stability derivative	Rotation through angle α
$C_{L_{\dot\alpha}}$	$C_{L_{\dot\alpha}}{}'$	$C_{L_{\dot\alpha}}$	$C_{L_{\dot\alpha}}{}''$	$C_{L_{\dot\alpha}}{}'$ (approx.)
$C_{m_{\dot\alpha}}$	$C_{m_{\dot\alpha}}{}'$	$C_{m_{\dot\alpha}} + \dfrac{\bar{x}}{c} C_{L_{\dot\alpha}}$	$C_{m_{\dot\alpha}}{}''$	$C_{m_{\dot\alpha}}{}'$

[1] The values of the stability derivatives in this column (origin at (0,0,0)) may be obtained from figures 7 and 8.
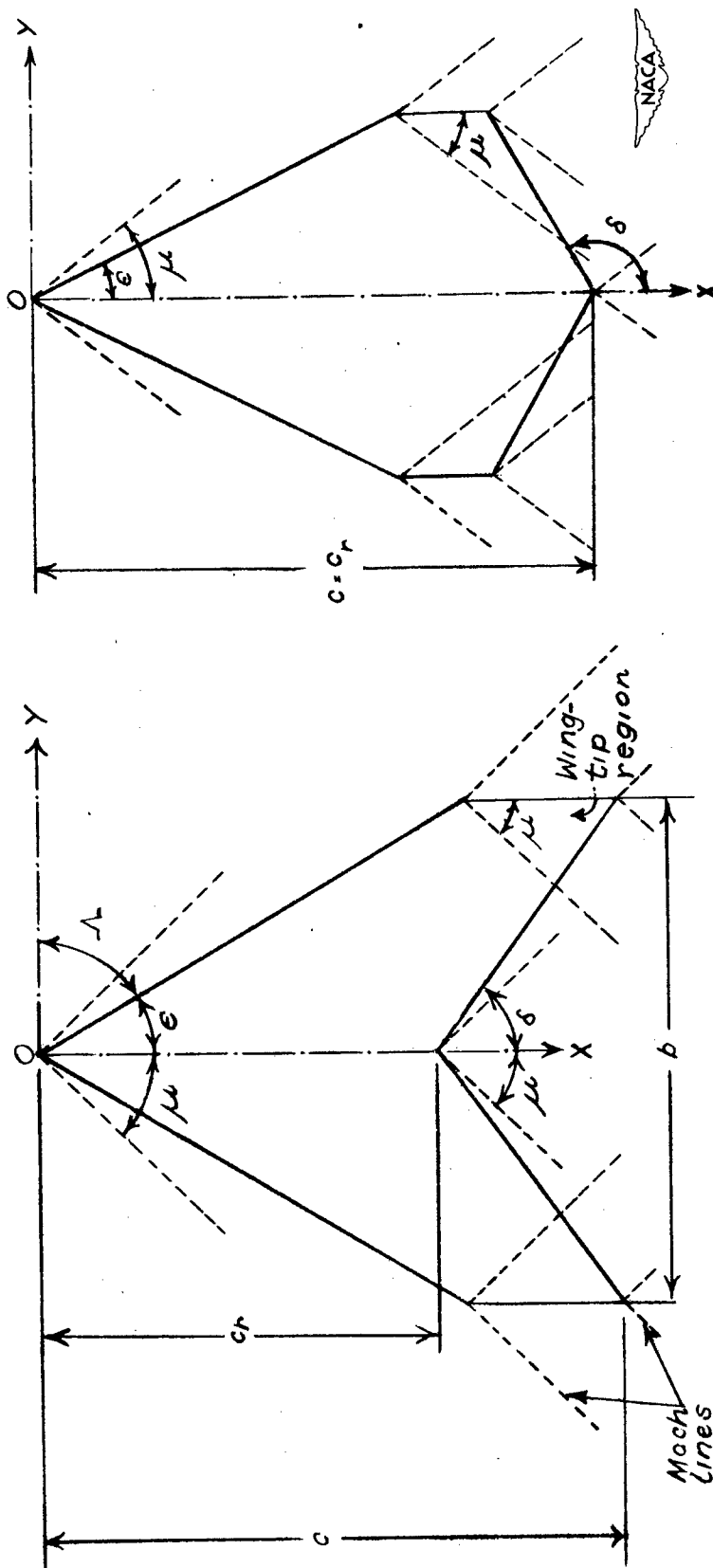
(a) Sweptback trailing edges.   (b) Sweptforward trailing edges.

Figure 1.- Sweptback wing with streamwise tips and sweptback or swept-
forward trailing edges. (Note that trailing edge is always inclined
at an angle of attack greater than the Mach angle.)
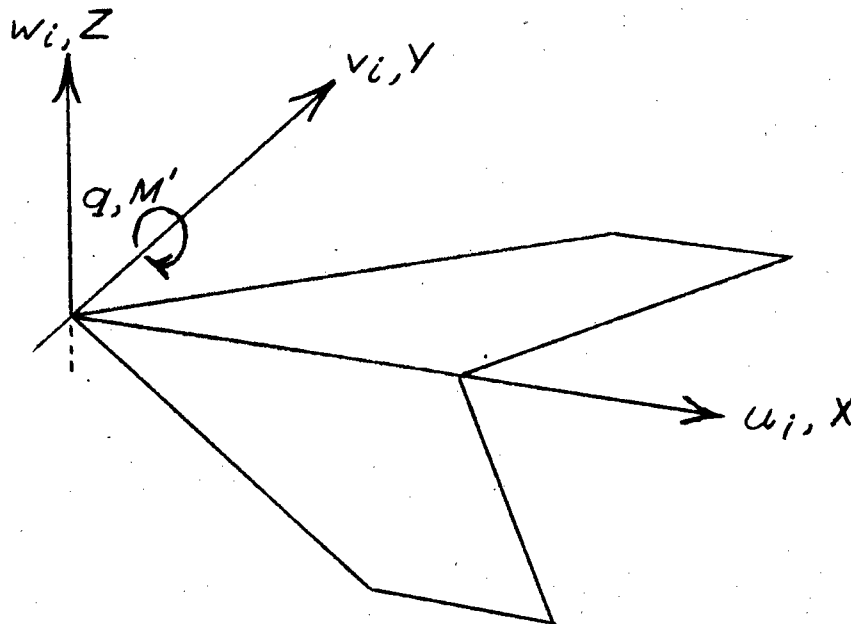
(a) Notation and body axes used in analysis.
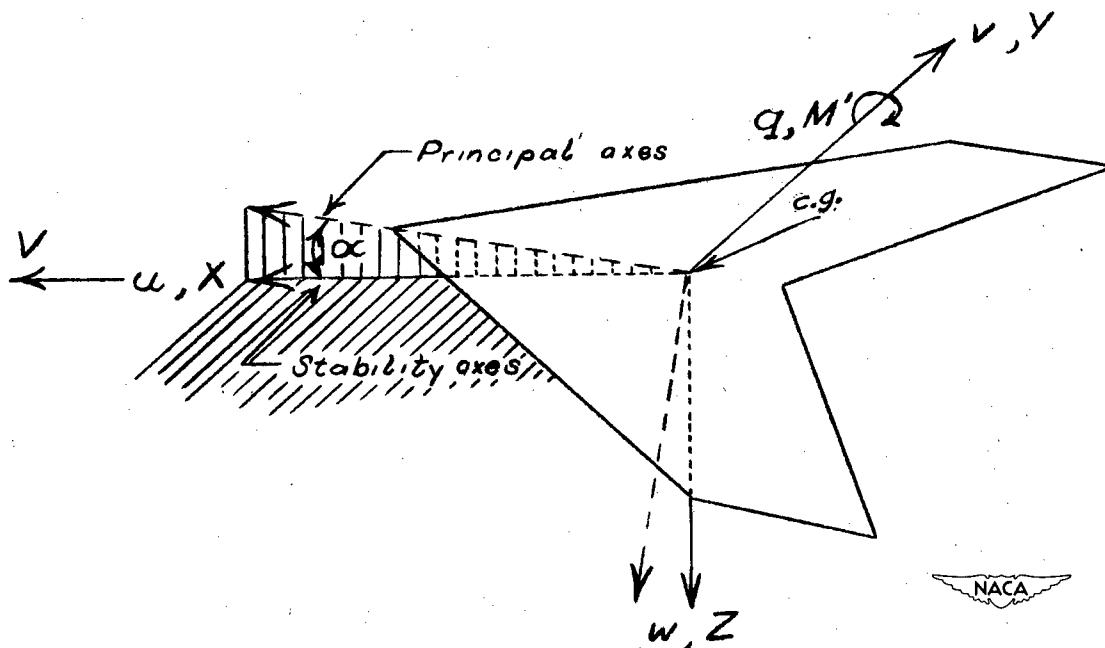
(b) Stability axes. Velocity, force, and moment arrangement in principal
    body axes system is the same as that of stability axes system.
    (Principal body axes dashed in for comparison.)

Figure 2.- System of axes and associated data.
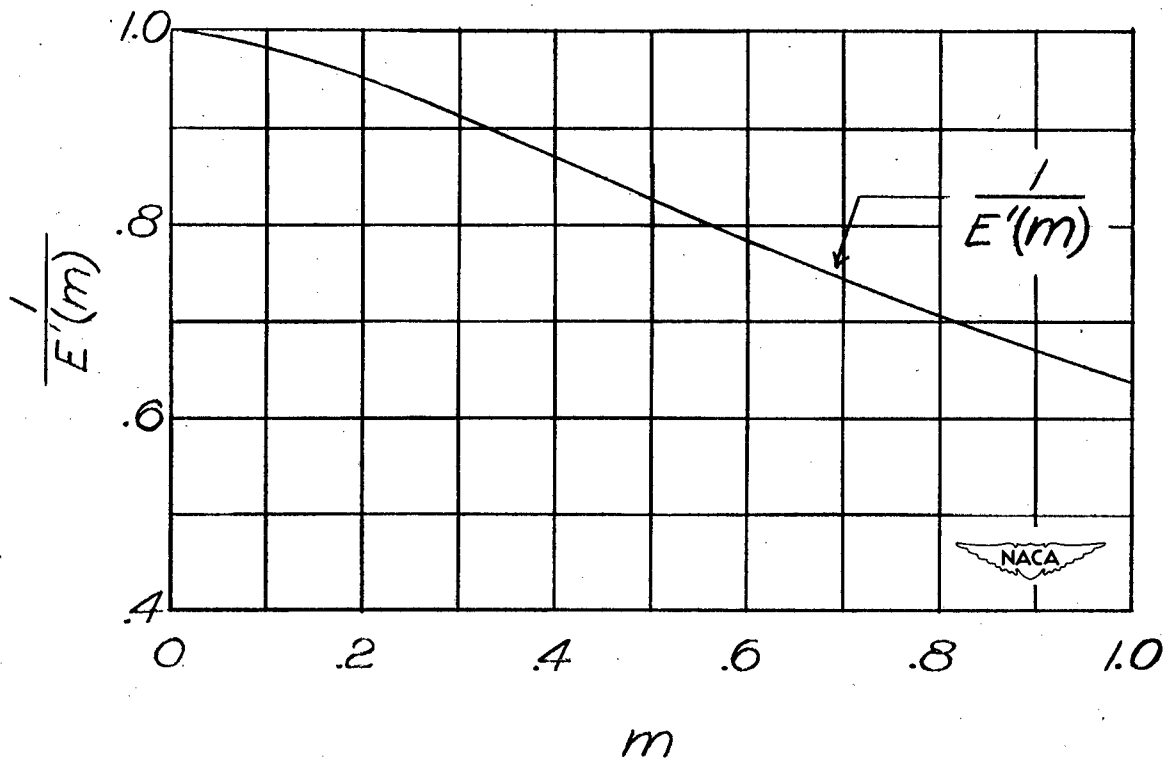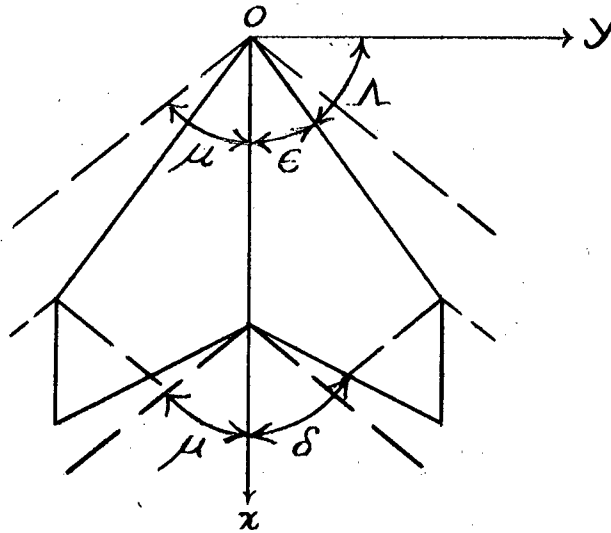
Figure 3.- Variation of the elliptic integral factor $\dfrac{1}{E'(m)}$ with $m = \dfrac{\tan \epsilon}{\tan \mu}$.

Equation of eg: $\quad x = B\left(\dfrac{b}{2} - y\right) + \dfrac{b}{2\theta_0}$

Equation of hf: $\quad x = \dfrac{y + c_r \tan \delta}{\tan \delta}$

Intersection of eg and hf:

$$y = \frac{\left(Bb\theta_0 - 2c_r\theta_0 + b\right)\tan \delta}{2\theta_0(B \tan \delta + 1)}$$
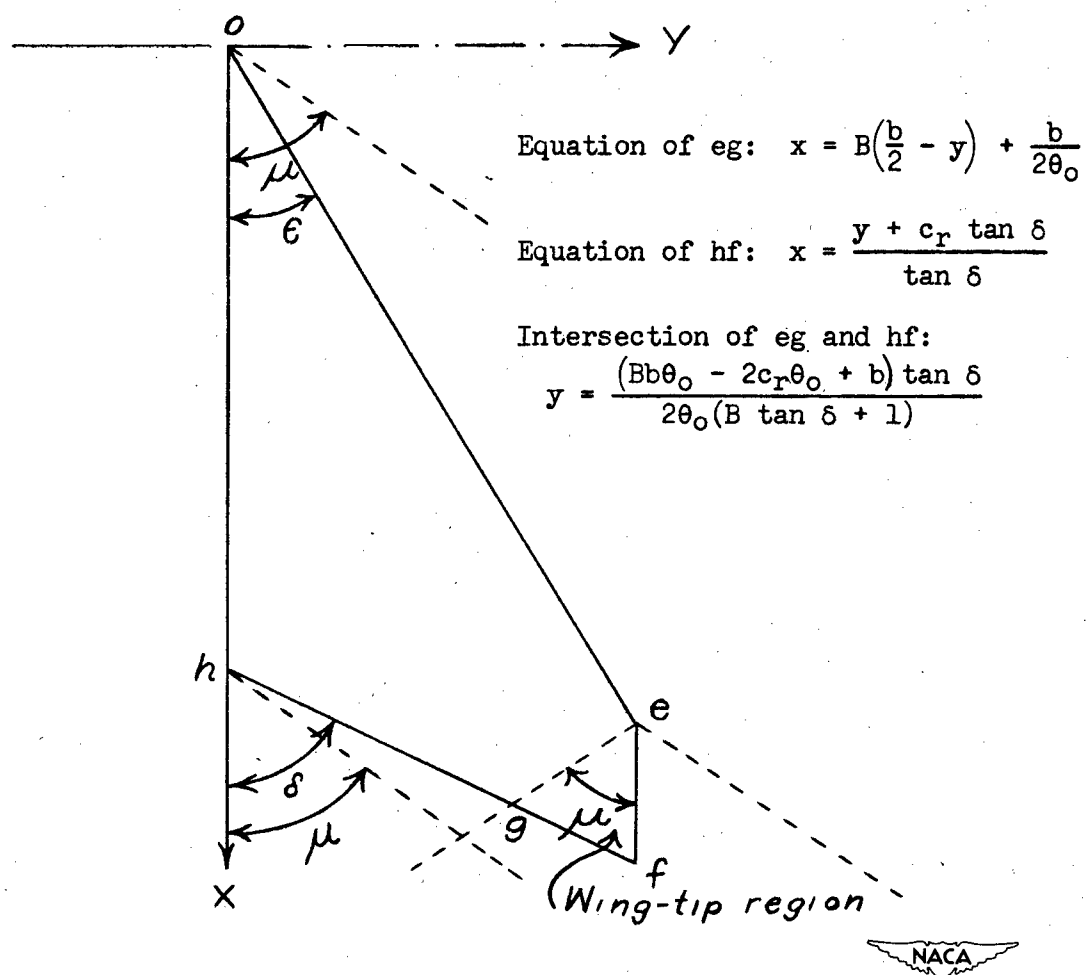
Figure 4.- Sketch of right panel of wing and associated data defining
limits of integration for the evaluation of forces and moments.

(a) Subsonic leading edge, super-   (b) Subsonic leading edge,   (c) Sonic leading edge, super-
    sonic trailing edge.   sonic trailing edge.   sonic trailing edge.
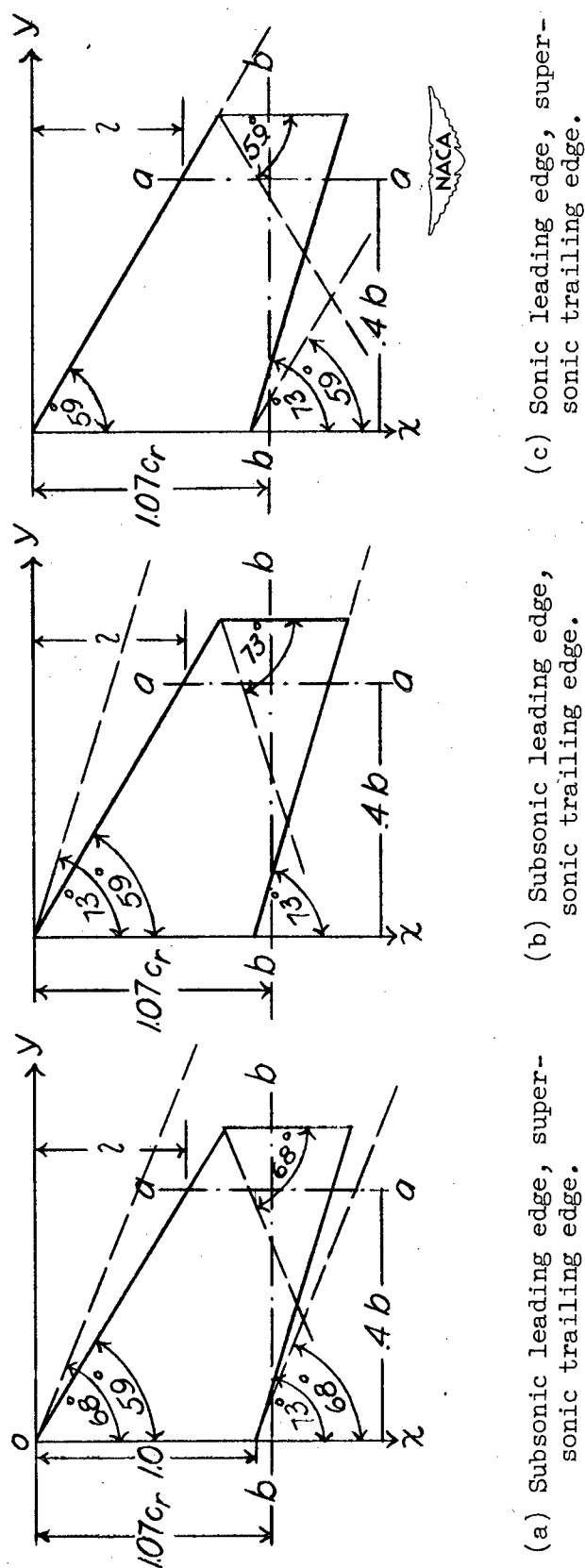
Figure 5.- Sketch of wing plan form for which the distribution of lifting pressure along sectional
            planes a-a and b-b was determined for three Mach line configurations.
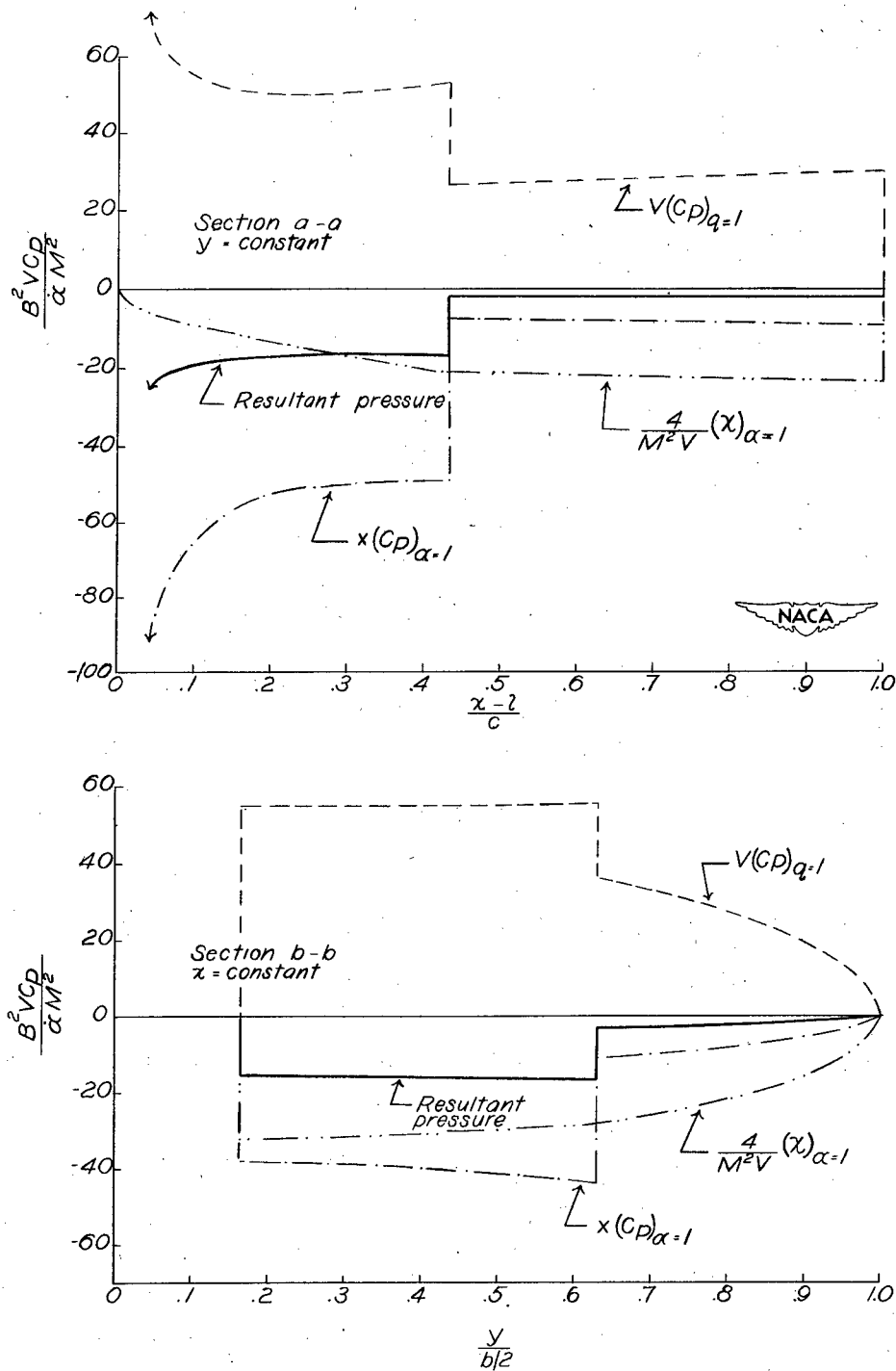
(a) Subsonic leading edge, supersonic trailing edge.

Figure 6.- Chordwise and spanwise pressure distributions along sectional
planes through the wing-tip region.
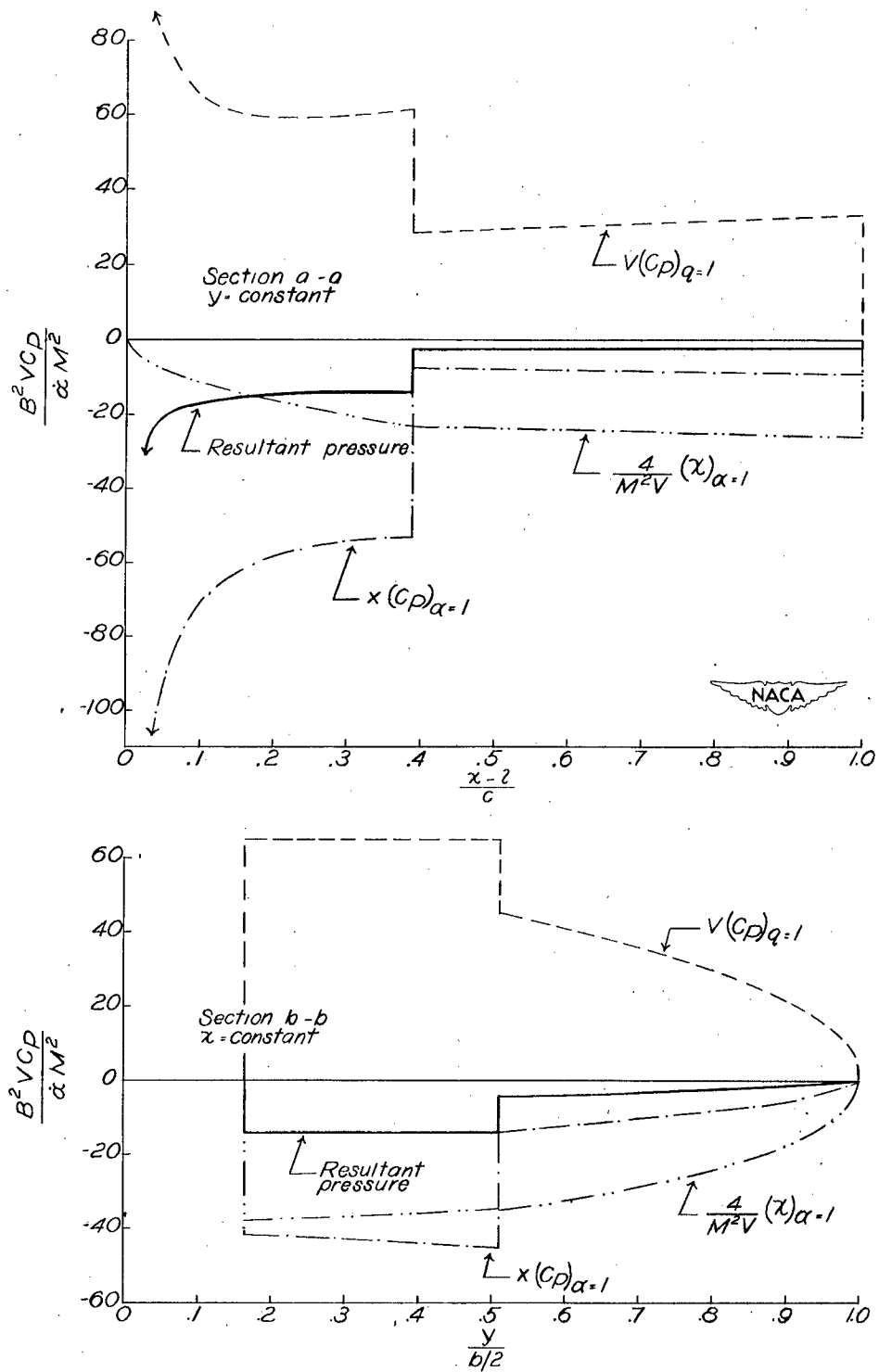
(b) Subsonic leading edge, sonic trailing edge.

Figure 6.- Continued.
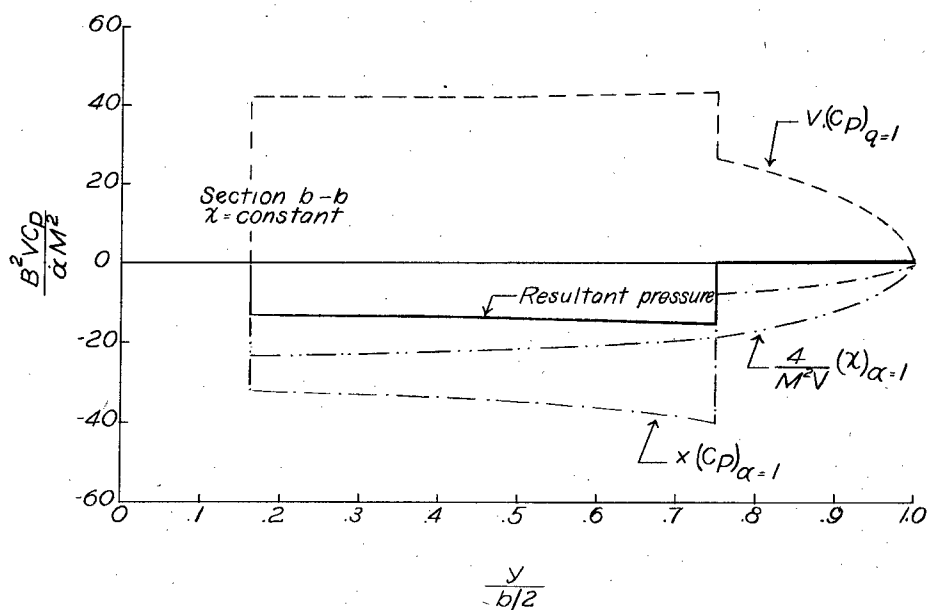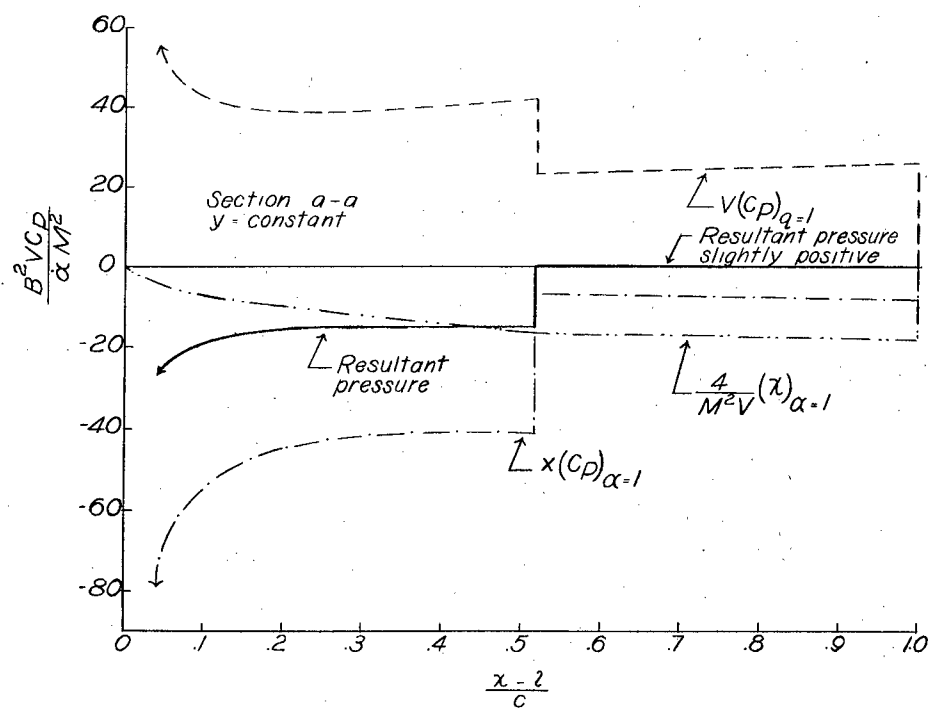
(c) Sonic leading edge, supersonic trailing edge.

Figure 6.- Concluded.
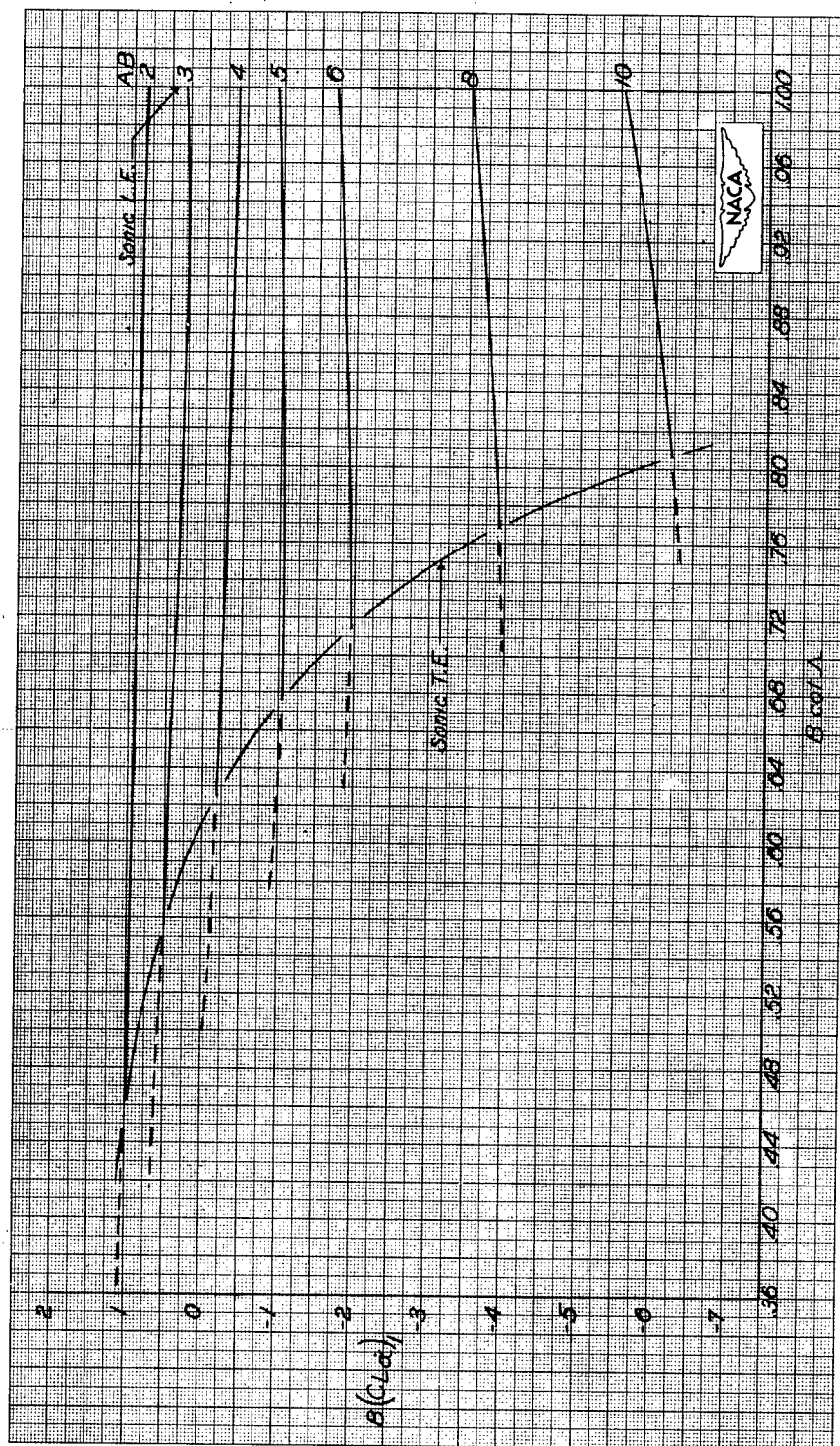
(a) $\lambda = 0.25$.

Figure 7.- Variation of $B\left(C_{L_\alpha}\right)_1$ and $B\left(C_{L_\alpha}\right)_2$ with $B \cot \Lambda$ for various values of AB and λ. Body axes system, origin at apex of wing. Dashed portions of curves have limited significance (see "Results and Discussion").
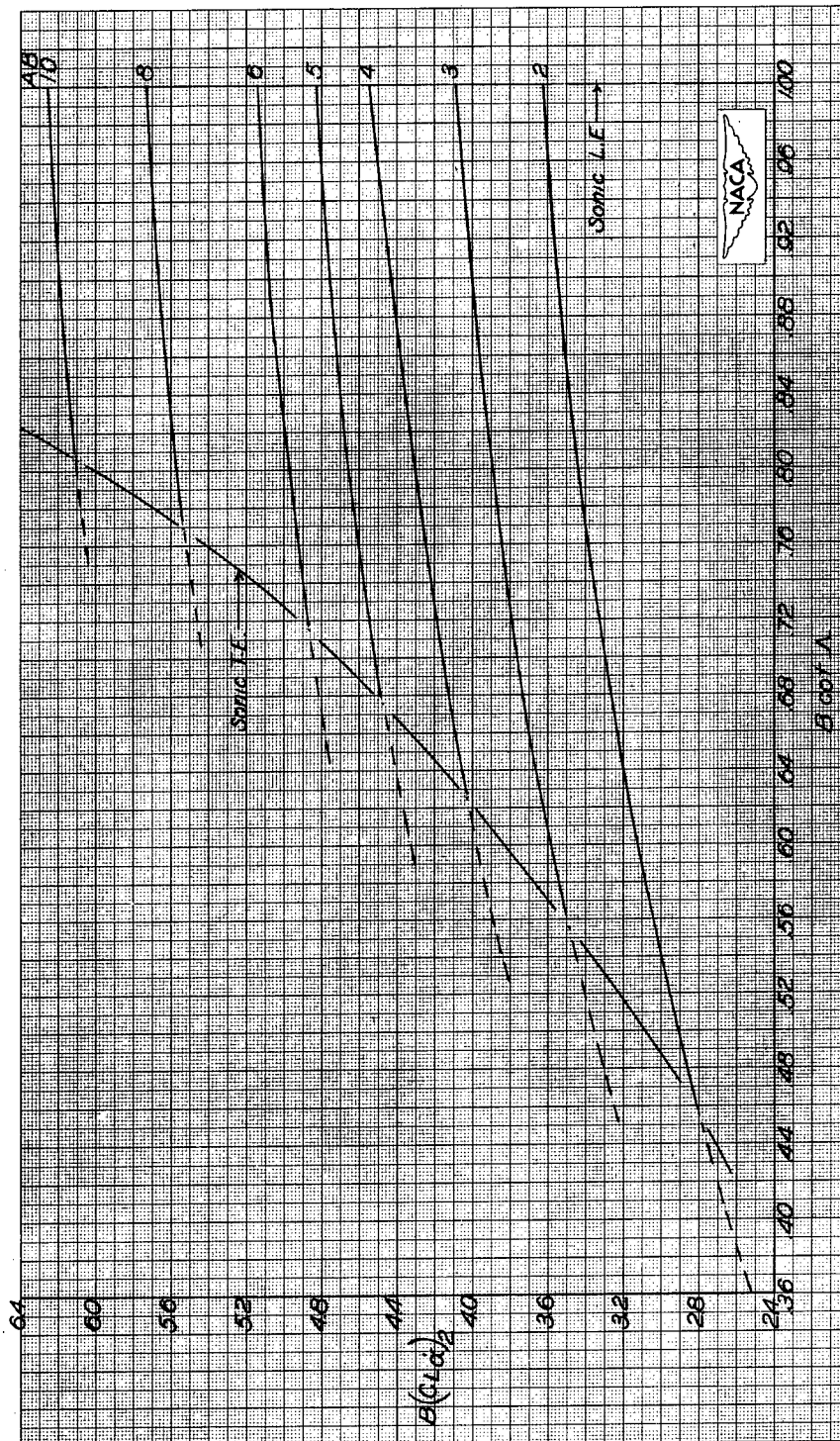
(a) Concluded. λ = 0.25.

Figure 7.- Continued.

(b) λ = 0.50.
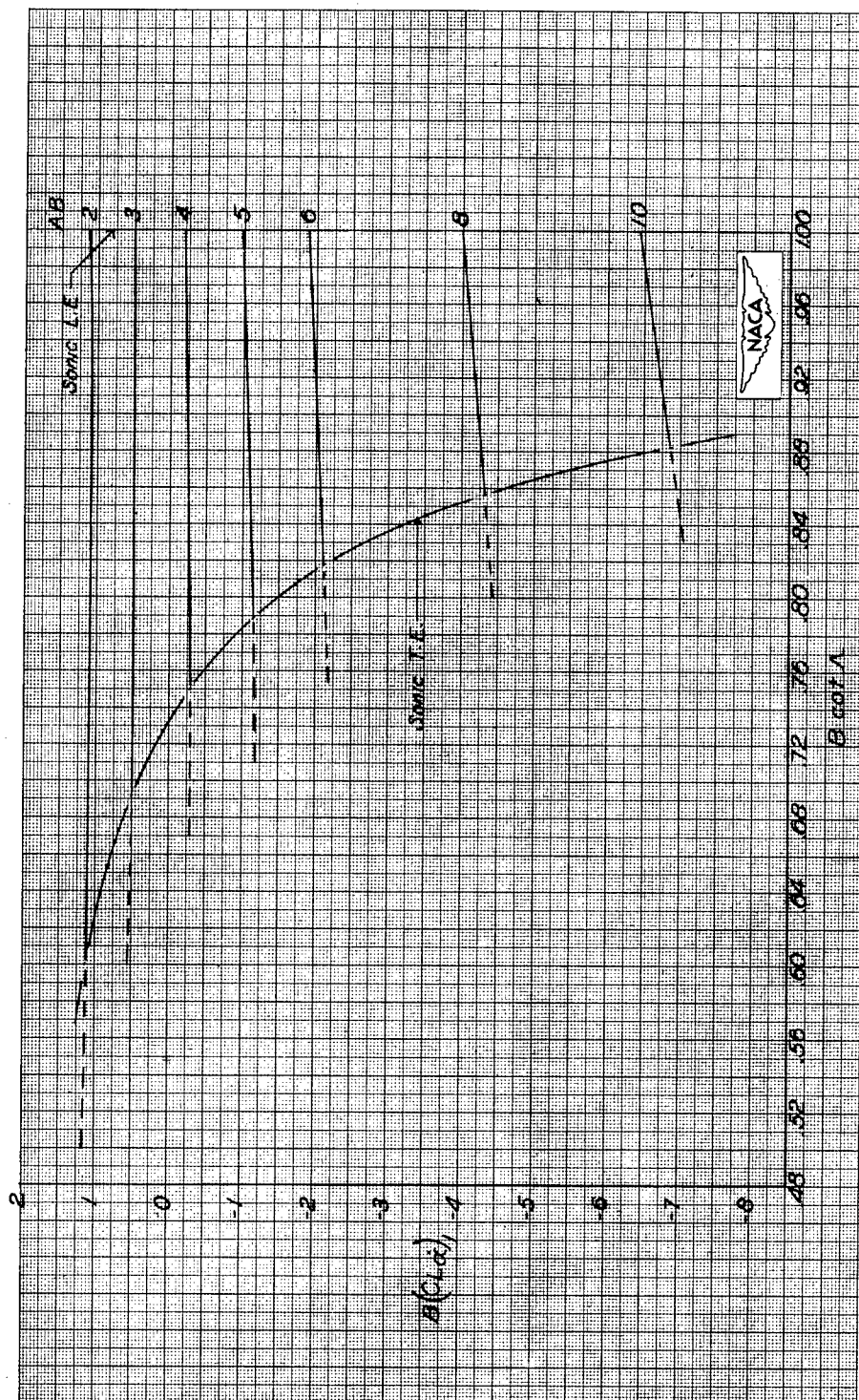
Figure 7.- Continued.
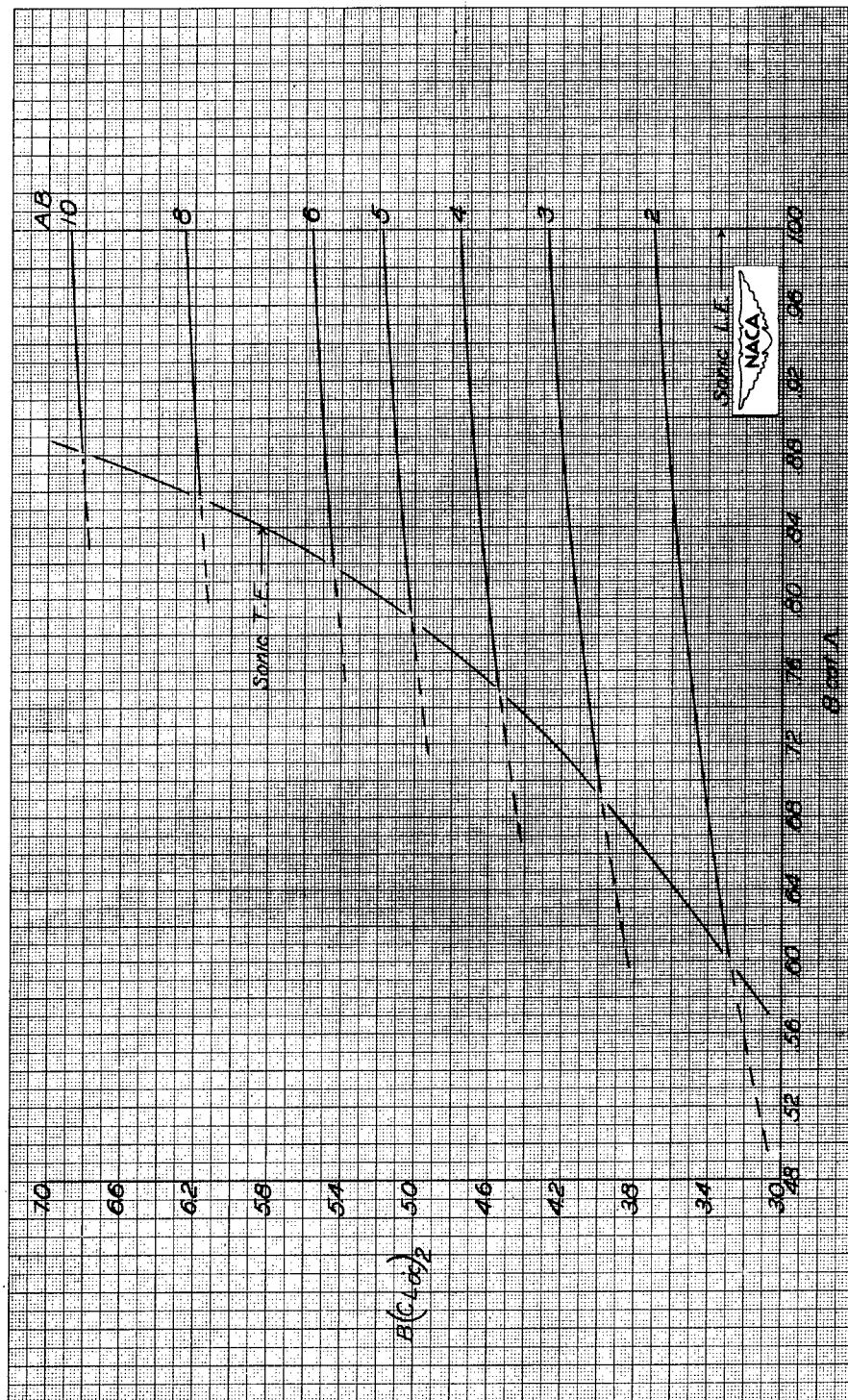
(b) Concluded.   λ = 0.50.

Figure 7.- Continued.

(c) $\lambda = 0.75$.

Figure 7.- Continued.
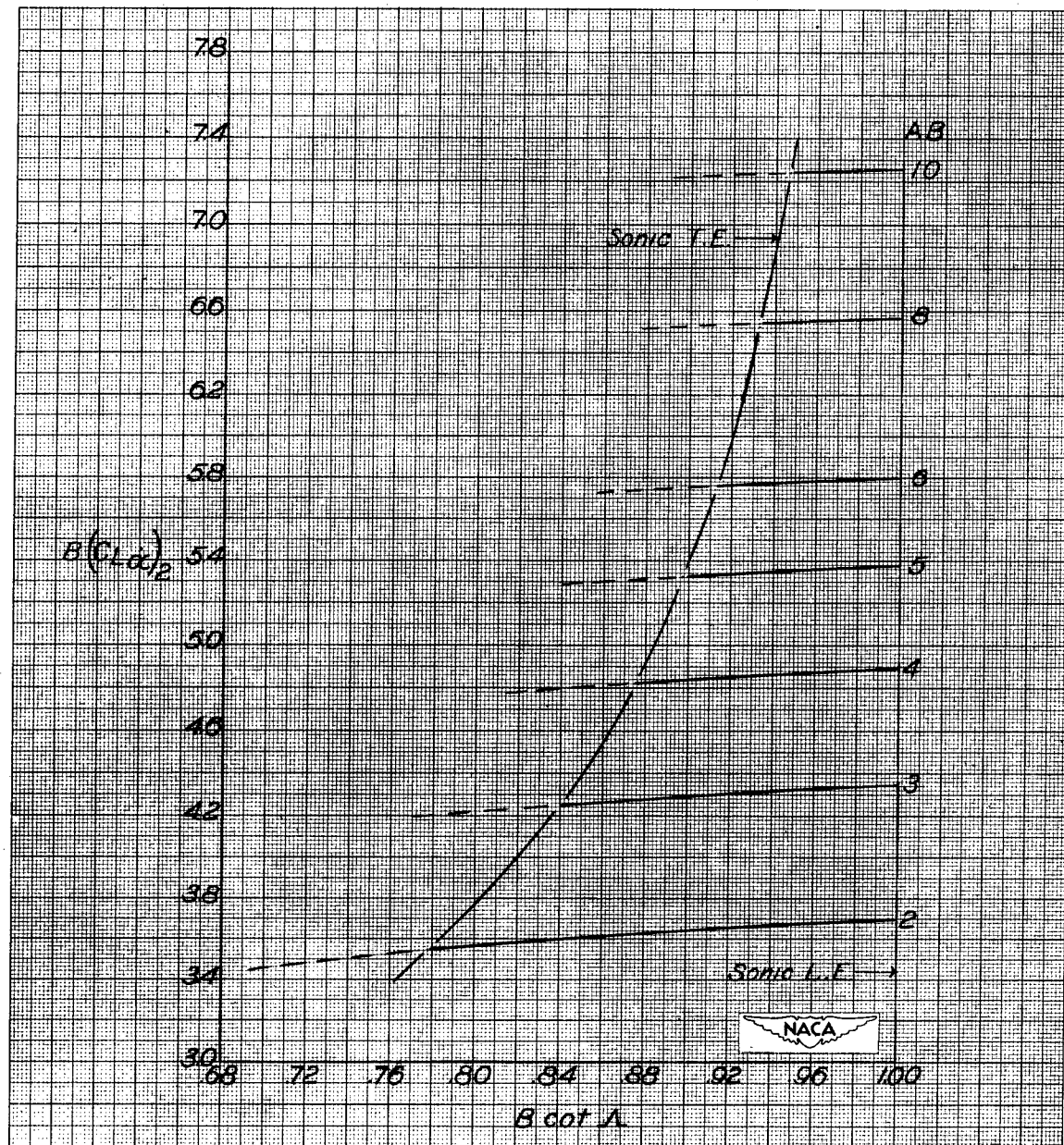
(c.) Concluded. $\lambda = 0.75$.

Figure 7.- Concluded.

(a) $\lambda = 0.25$.

Figure 8.- Variation of $B\left(C_{m_{\dot{\alpha}}}\right)_1$ and $B\left(C_{m_{\dot{\alpha}}}\right)_2$ with $B \cot \Lambda$ for various values of AB and λ. Body axes system, origin at apex of wing. Dashed portions of curves have limited significance (see "Results and Discussion").
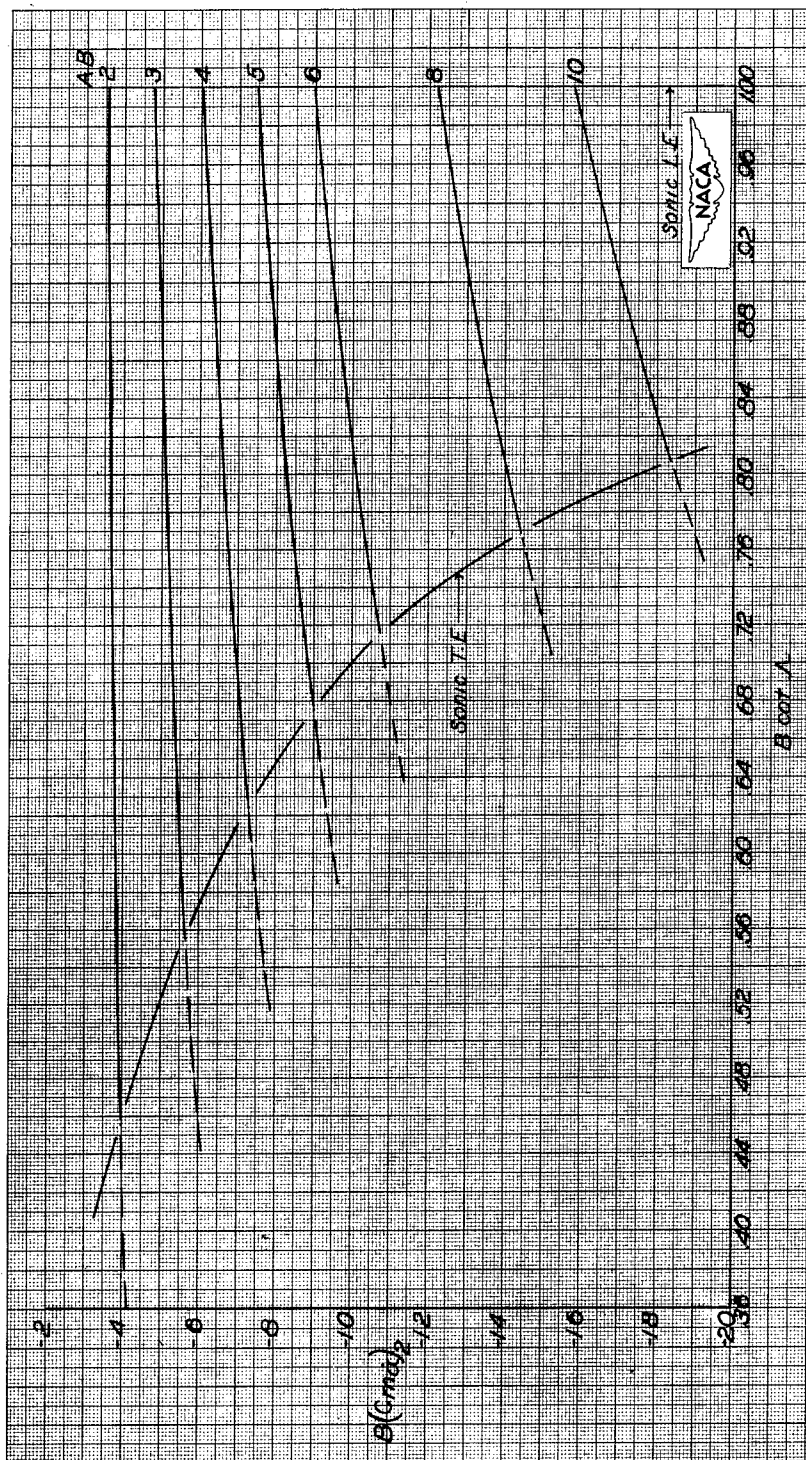
(a) Concluded. λ = 0.25.

Figure 8.– Continued.
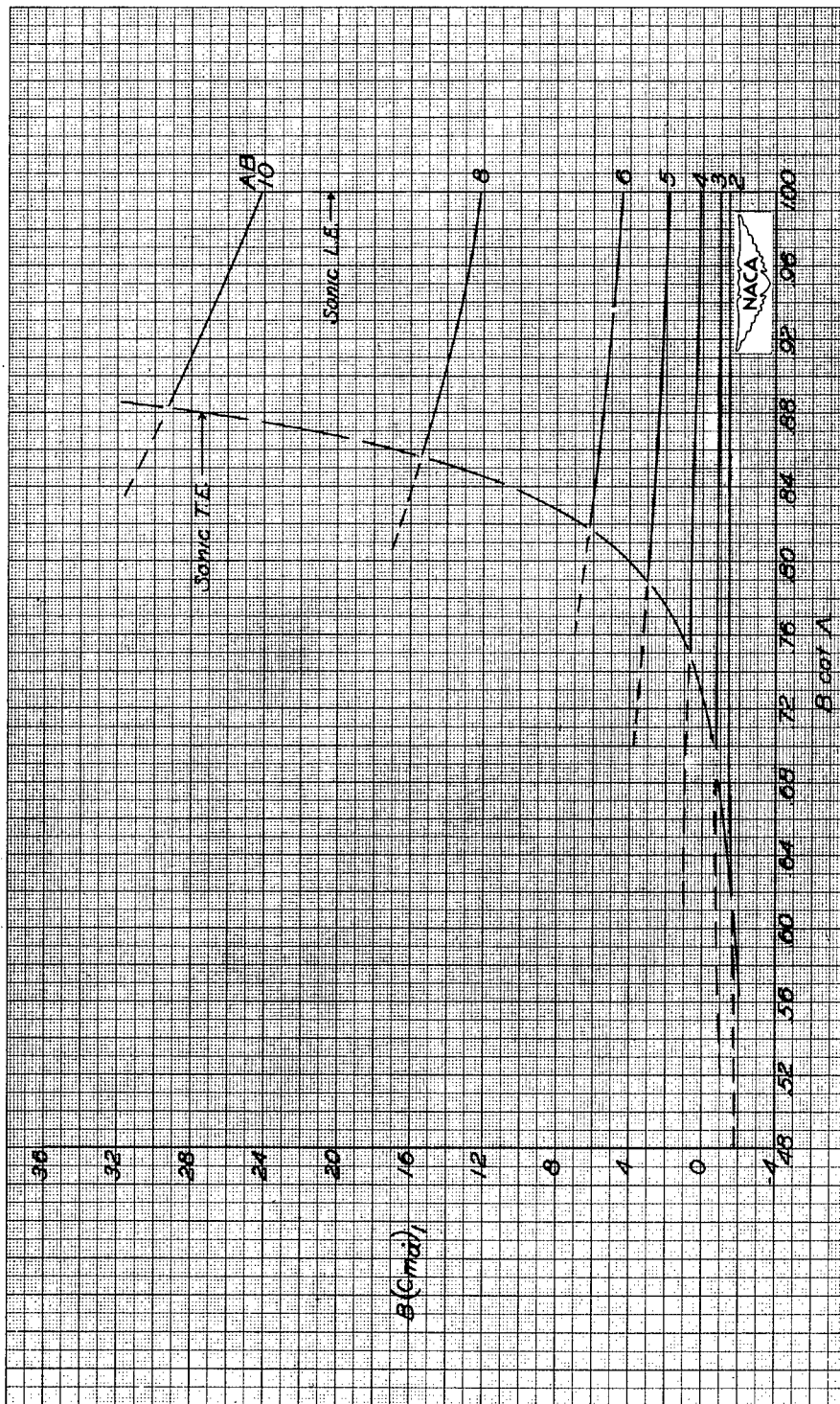
(b) $\lambda = 0.50.$

Figure 8.- Continued.
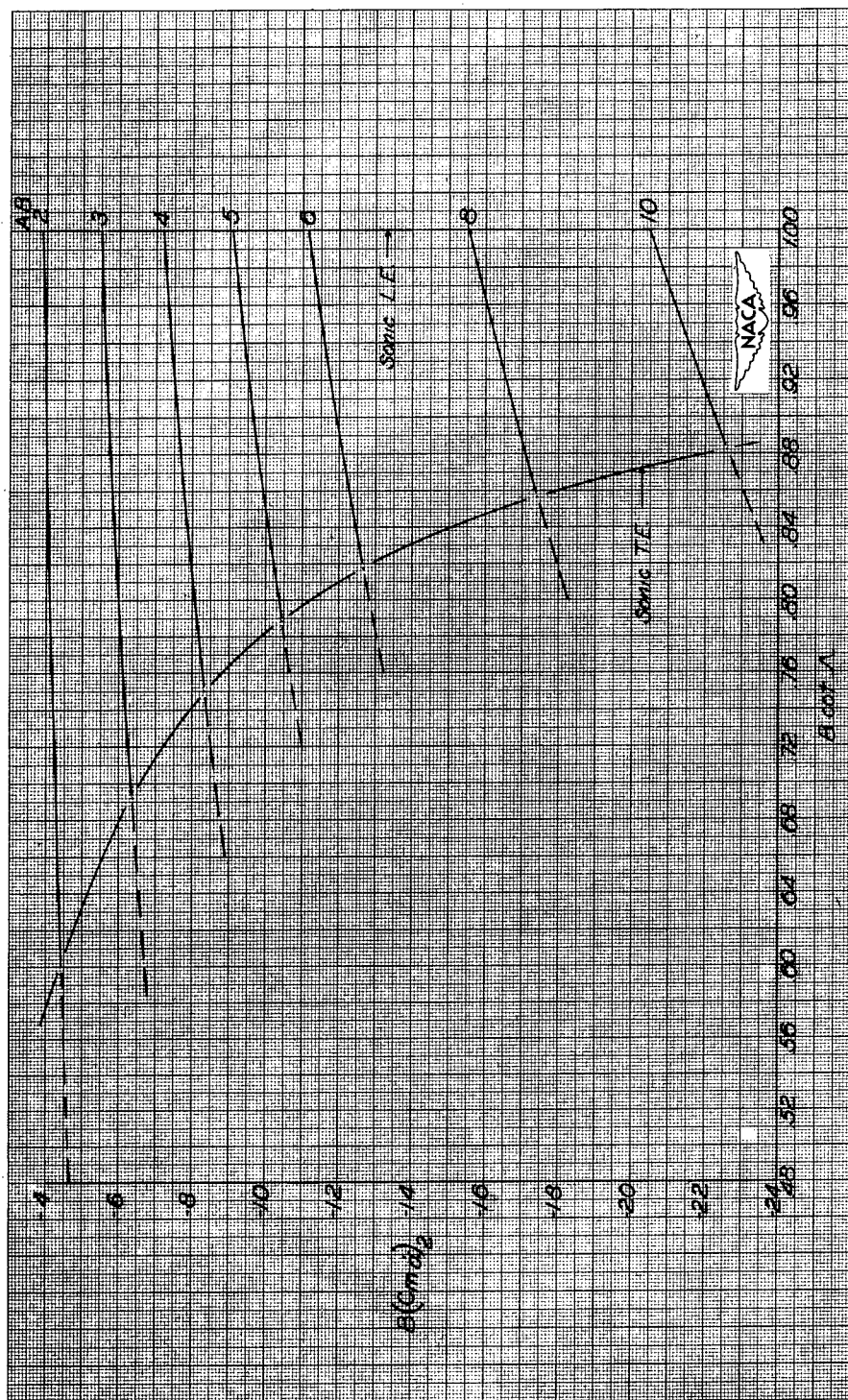
(b) Concluded. $\lambda = 0.50$.

Figure 8.- Continued.
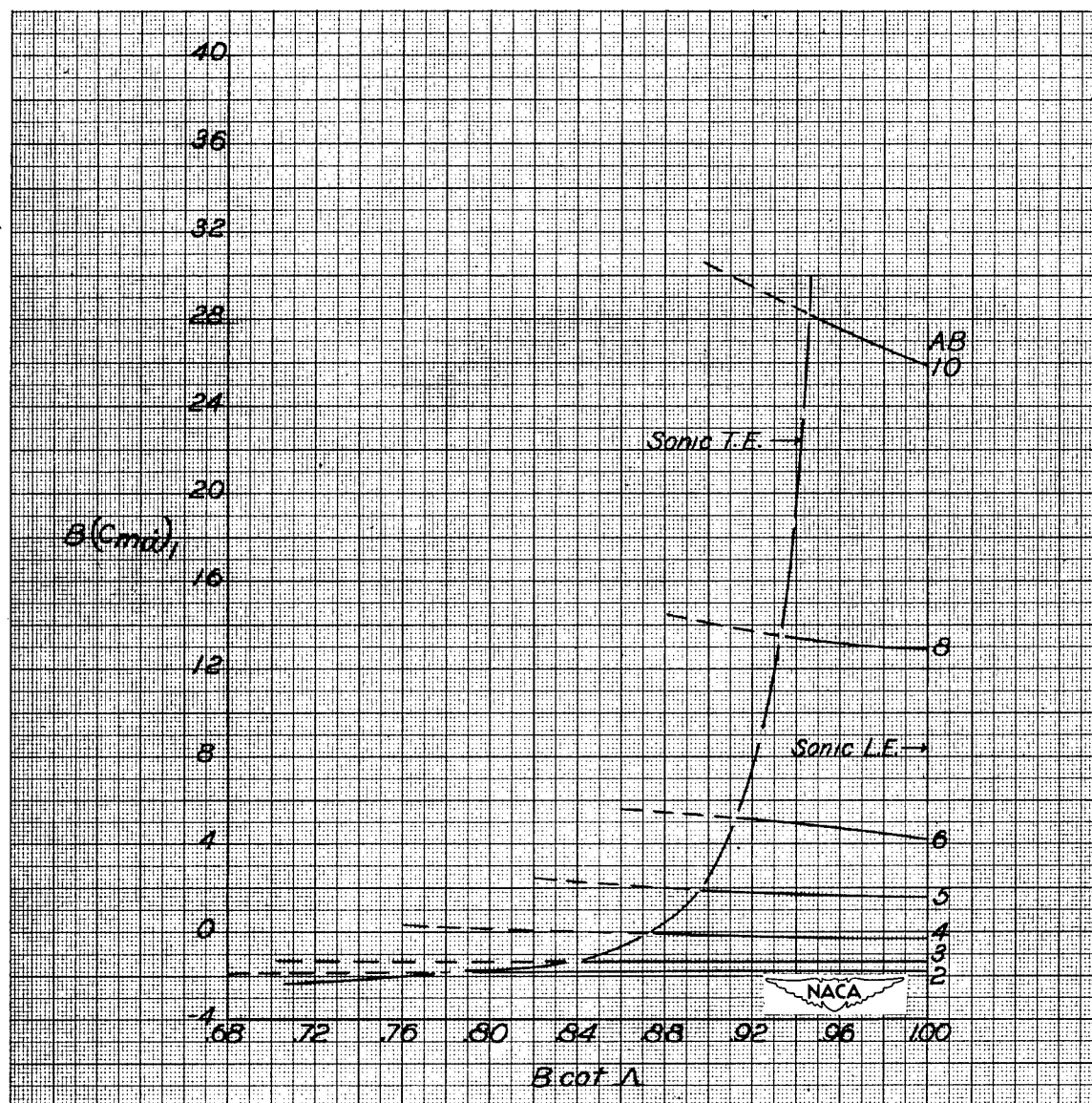
(c) $\lambda = 0.75$.

Figure 8.- Continued.
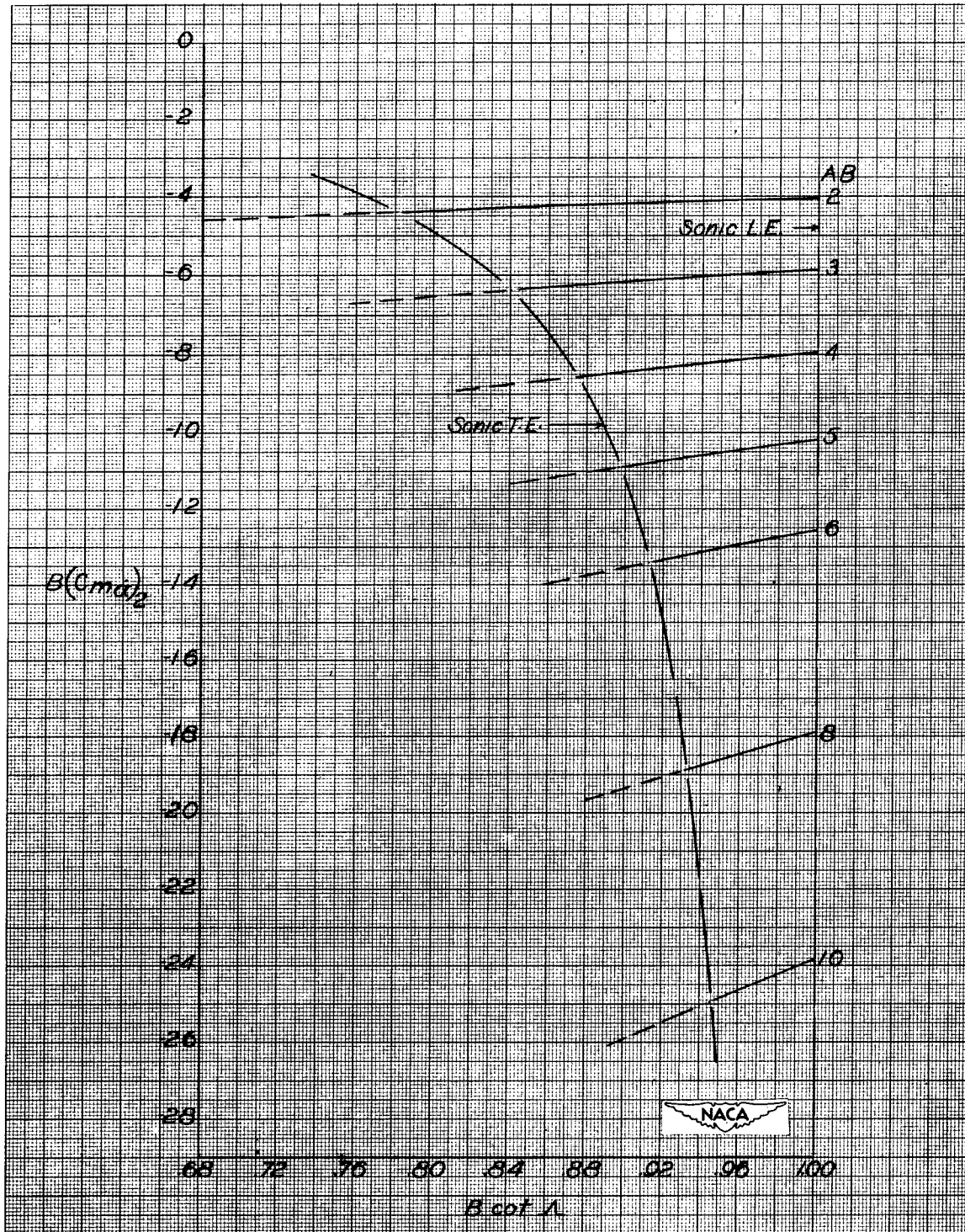
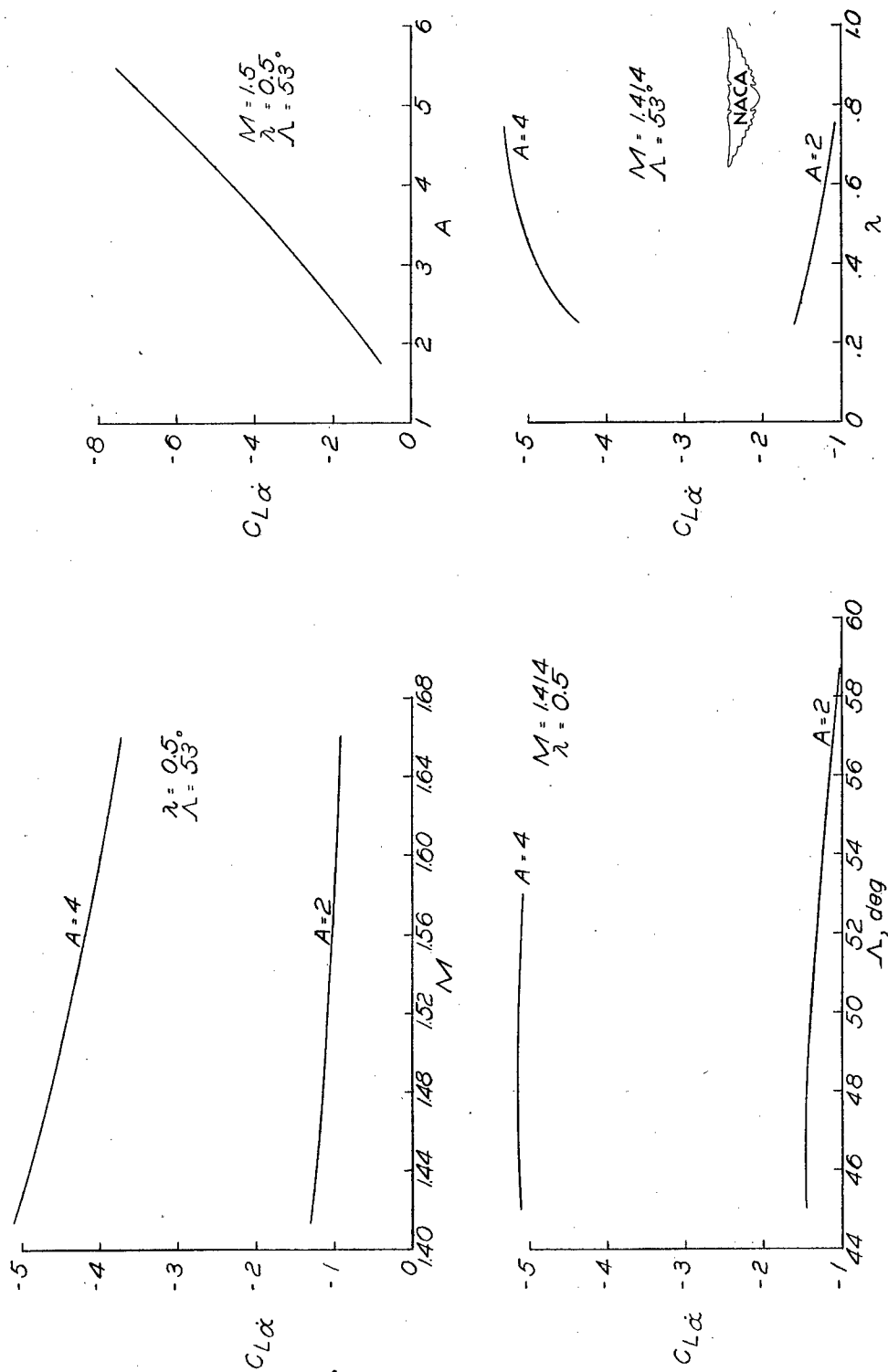(c) Concluded. $\lambda = 0.75$.

Figure 8.- Concluded.

Figure 9.- Some illustrative variations of $C_{L_{\dot\alpha}}$ with Mach number, aspect ratio, sweepback, and taper ratio. Stability axes system; static margin, 0.05.
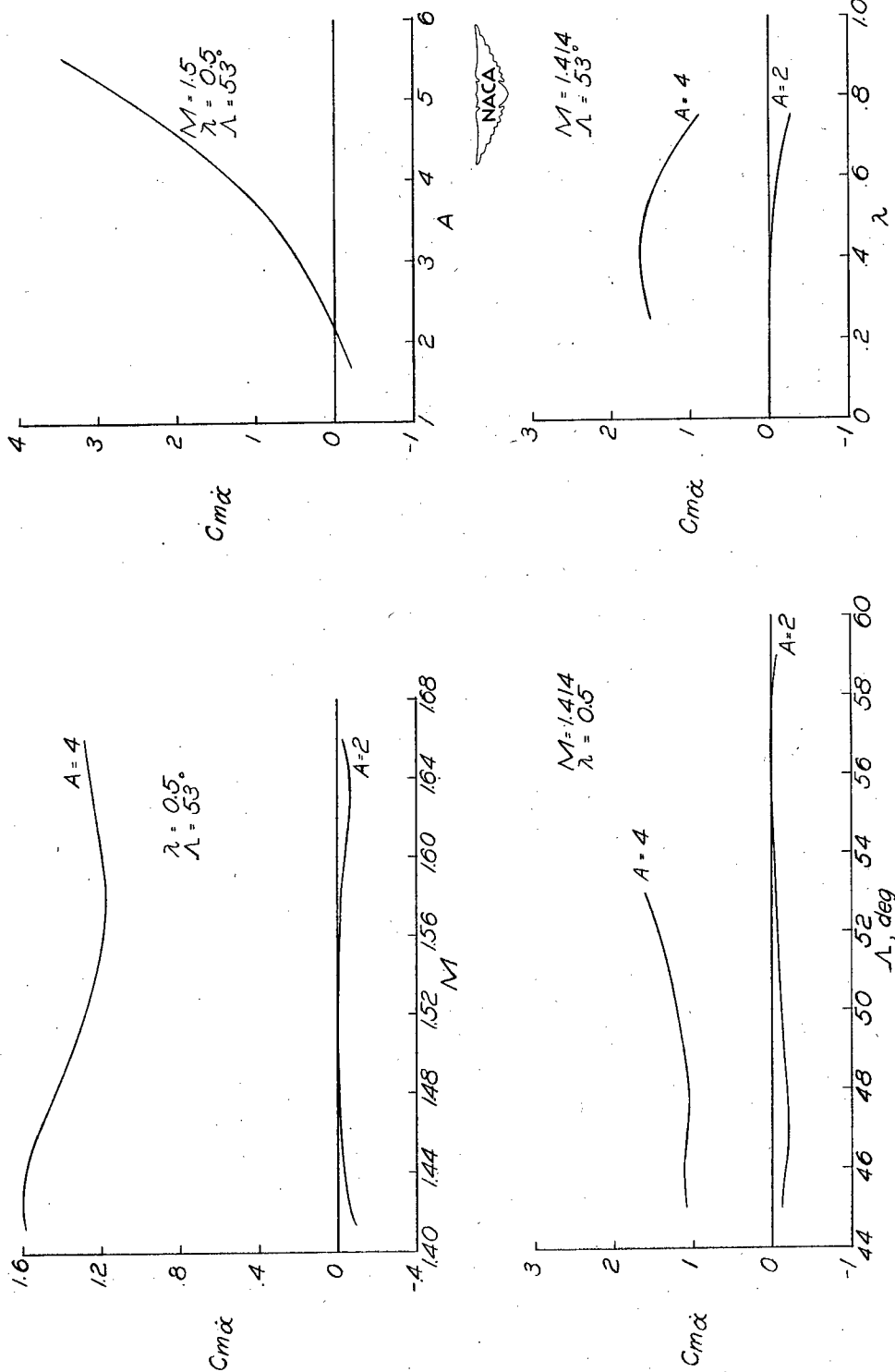
Figure 10.- Some illustrative variations of $C_{m_{\dot{\alpha}}}$ with Mach number, aspect ratio, sweepback, and taper ratio. Stability axes system; static margin, 0.05.

1.2.2.2.2

Wings, Complete -
Aspect Ratio

NACA

Supersonic Lift and Pitching Moment of Thin Sweptback
Tapered Wings Produced by Constant Vertical
Acceleration. Subsonic Leading Edges and Supersonic
Trailing Edges.

By Frank S. Malvestuto, Jr., and Dorothy M. Hoover

NACA TN 2315
March 1951

(Abstract on Reverse Side)

1.2.2.2.4

Wings, Complete -
Taper and Twist

NACA

Supersonic Lift and Pitching Moment of Thin Sweptback
Tapered Wings Produced by Constant Vertical
Acceleration. Subsonic Leading Edges and Supersonic
Trailing Edges.

By Frank S. Malvestuto, Jr., and Dorothy M. Hoover

NACA TN 2315
March 1951

(Abstract on Reverse Side)

1.2.2.1

Wings, Complete - Theory

NACA

Supersonic Lift and Pitching Moment of Thin Sweptback
Tapered Wings Produced by Constant Vertical
Acceleration. Subsonic Leading Edges and Supersonic
Trailing Edges.

By Frank S. Malvestuto, Jr., and Dorothy M. Hoover

NACA TN 2315
March 1951

(Abstract on Reverse Side)

1.2.2.2.3

Wings, Complete - Sweep

NACA

Supersonic Lift and Pitching Moment of Thin Sweptback
Tapered Wings Produced by Constant Vertical
Acceleration. Subsonic Leading Edges and Supersonic
Trailing Edges.

By Frank S. Malvestuto, Jr., and Dorothy M. Hoover

NACA TN 2315
March 1951

(Abstract on Reverse Side)

Abstract

Based upon time-dependent linearized supersonic flow, theoretical approximations to the lift C_{L_α} and pitching moment C_{m_α} produced by constant vertical accelerations were derived for a series of sweptback tapered wings with streamwise tips. The results are applicable for a range of Mach number for which the wing is wholly contained between the Mach cones springing from the nose and apex of the trailing edge of the wing.

Design curves are presented which permit rapid estimations of C_{L_α} and C_{m_α} for given values of aspect ratio, taper ratio, Mach number, and leading-edge sweep.

Abstract

Based upon time-dependent linearized supersonic flow, theoretical approximations to the lift C_{L_α} and pitching moment C_{m_α} produced by constant vertical accelerations were derived for a series of sweptback tapered wings with streamwise tips. The results are applicable for a range of Mach number for which the wing is wholly contained between the Mach cones springing from the nose and apex of the trailing edge of the wing.

Design curves are presented which permit rapid estimations of C_{L_α} and C_{m_α} for given values of aspect ratio, taper ratio, Mach number, and leading-edge sweep.

Abstract

Based upon time-dependent linearized supersonic flow, theoretical approximations to the lift C_{L_α} and pitching moment C_{m_α} produced by constant vertical accelerations were derived for a series of sweptback tapered wings with streamwise tips. The results are applicable for a range of Mach number for which the wing is wholly contained between the Mach cones springing from the nose and apex of the trailing edge of the wing.

Design curves are presented which permit rapid estimations of C_{L_α} and C_{m_α} for given values of aspect ratio, taper ratio, Mach number, and leading-edge sweep.

Abstract

Based upon time-dependent linearized supersonic flow, theoretical approximations to the lift C_{L_α} and pitching moment C_{m_α} produced by constant vertical accelerations were derived for a series of sweptback tapered wings with streamwise tips. The results are applicable for a range of Mach number for which the wing is wholly contained between the Mach cones springing from the nose and apex of the trailing edge of the wing.

Design curves are presented which permit rapid estimations of C_{L_α} and C_{m_α} for given values of aspect ratio, taper ratio, Mach number, and leading-edge sweep.

NACA TN 2315